**STAR JASON-2 AMR Study Report**

**Date: June, 2010**

## 1. Highlighted Areas

- AMSU-A and AMR SNO
- Linear Mapping between AMSU-A and AMR
- AMR Water Vapor and Cloud Liquid Water Retrievals
- AMR Algorithm Performance

## 2. Technical Descriptions

### 2.1 AMR and AMSU-A Simultaneous Nadir Over-passing (Changyong)

### 2.2 Linear Mapping between AMSU-A and AMR

#### 2.2.1 Dataset

AMR on board of Jason-2 that was launched on June, 20 2008 is a nadir viewing passive microwave instrument which collects radiation reflected by the oceans at frequencies of 18.7, 23.8 and 34 GHz with a spatial resolution near 25 km. In this study, AMR brightness temperatures at channel 23.8 and 34.0 GHz were used to retrieve total precipitable water and cloud liquid water for the period spanning from June 22, 2008 to Dec. 31, 2009. The same retrieval procedure will be used for 2010 data when most of the 2010 data become available in order to get more accurate mapping coefficients. There are three families of geophysical data records (GDRs) of Jason-2 products in NetCDF format, distinguished by increasing latency and

accuracy, going from the operational GDR (OGDR, available 3-5 hours), to the Interim GDR (IGDR available 1-2 days), to the final GDR(available around 60 Days). The level 2 along track final GDR data were used here as it is most completed, accuracy and validated data. The data covers the entire Earth between 66.15°S to 66.15°N which is about global 95% unfrozen ocean environment.

### 2.2.2 Linear Mapping

Since the first launch of the Advanced Microwave Sounding Unit (AMSU) onboard NOAA-15, the products including cloud liquid, water vapor, rain rate, snow cover and sea ice concentration have been operationally generated by NOAA with a quality similar to those derived from SSM/I although the AMSU only has four window channels. Since AMR has two channels similar to AMSU-A, the operational AMSU water vapor and cloud algorithms can be directly used for AMR after channels are linearly mapped into AMSU-A channels. This linear mapping also calibrates AMR data using AMSU-A as a reference.

AMR on board JASON-2 and AMSU-A of Met-op Simultaneous Nadir Overpass (SNO see section 2.1) match up data is imported into excel files to get map, linear mapping coefficients and equations as follows:

For 2008: $Yamr = 1.0002Xamsu$ (both channels at 23.8 GHz)

$Yamr = 0.9778Xamsu$ (channels at 34.0 GHz and 31.4 GHz)

For 2009 $Yamr = 0.9991Xamsu$ (both channels at 23.8GHz)

$Yamr = 1.0246Xamsu$ (channels at 34.0 GHz and 31.4 GHz)

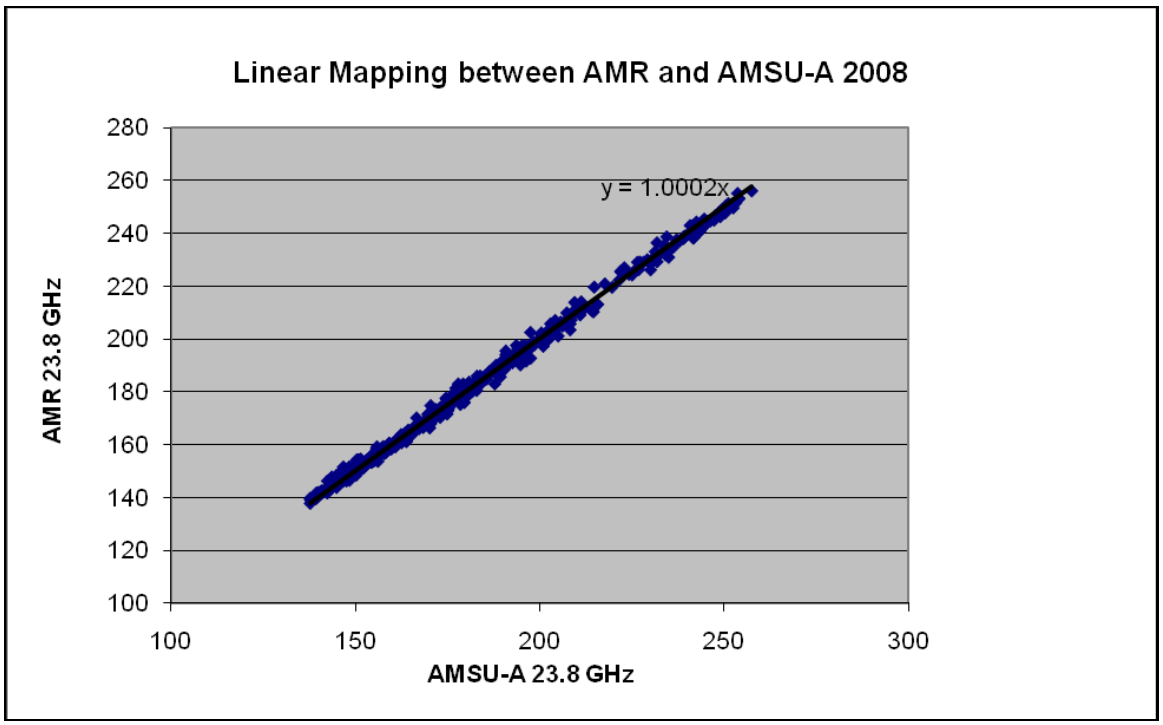
Linear Mapping between AMR and AMSU-A 2008
y = 1.0002x
AMR 23.8 GHz
AMSU-A 23.8 GHz
280
260
240
220
200
180
160
140
120
100
100
150
200
250
300

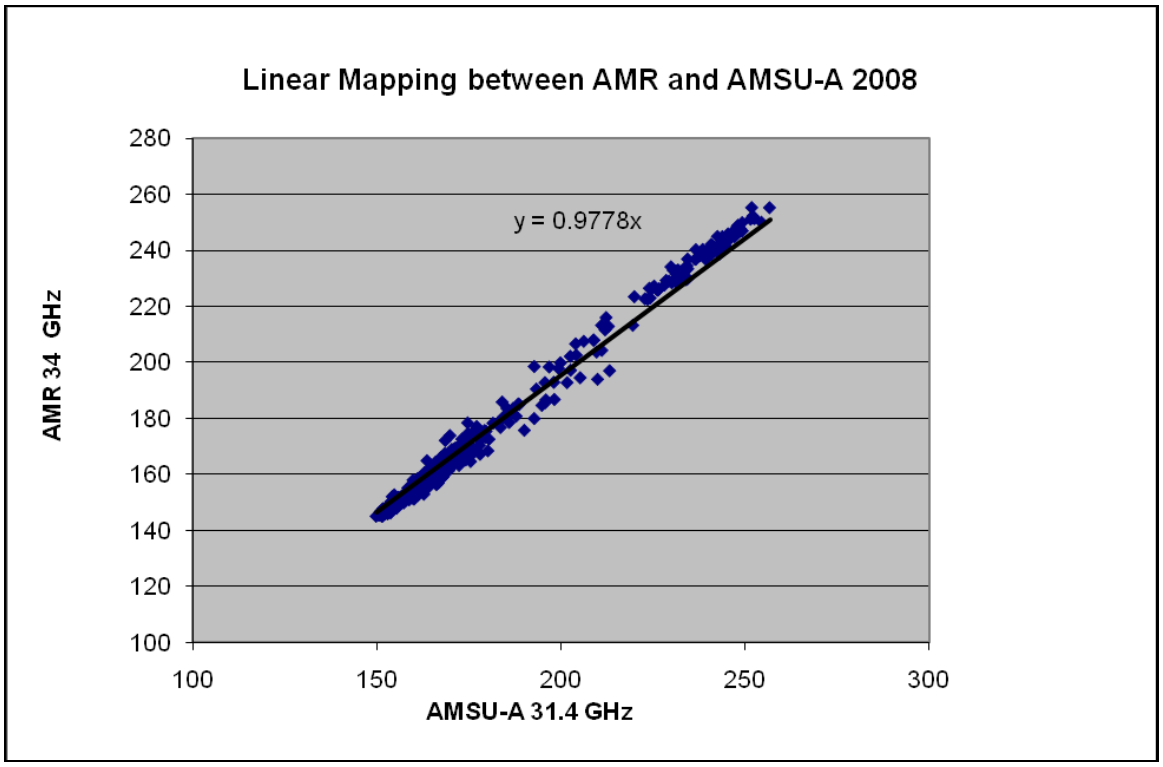
Linear Mapping between AMR and AMSU-A 2008
y = 0.9778x
AMR 34 GHz
AMSU-A 31.4 GHz
280
260
240
220
200
180
160
140
120
100
100
150
200
250
300

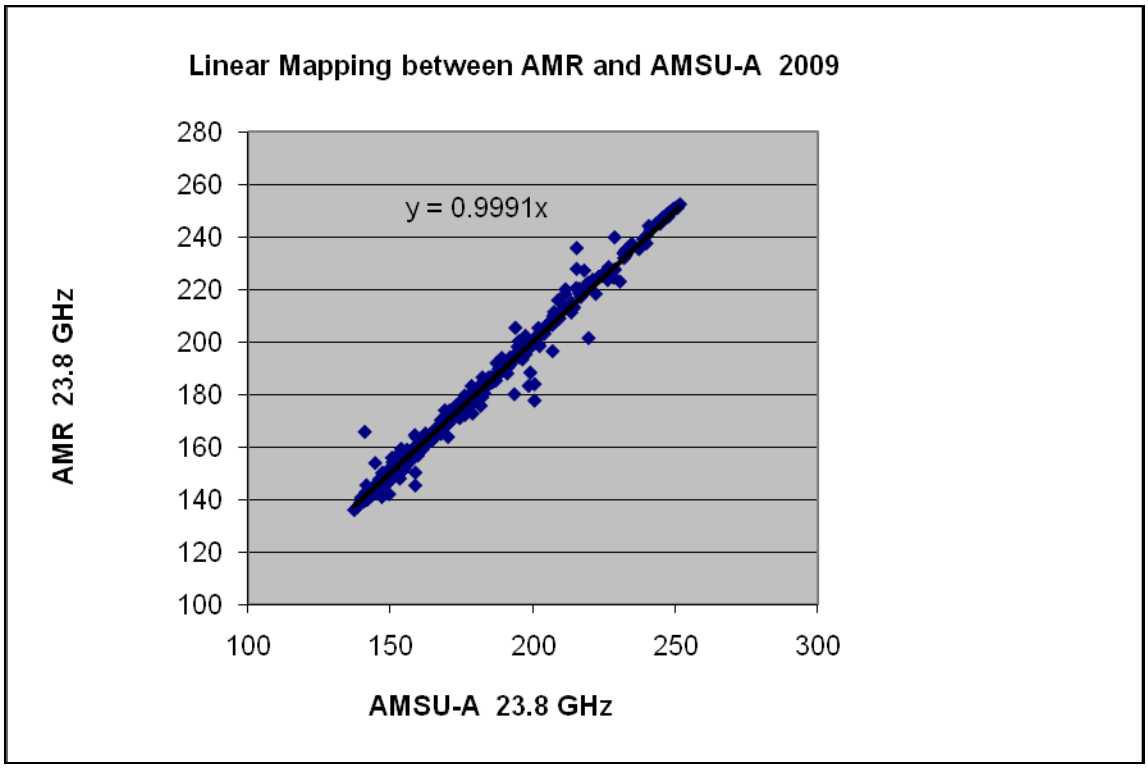
Linear Mapping between AMR and AMSU-A 2009
y = 0.9991x
AMR 23.8 GHz
AMSU-A 23.8 GHz
280
260
240
220
200
180
160
140
120
100
100
150
200
250
300

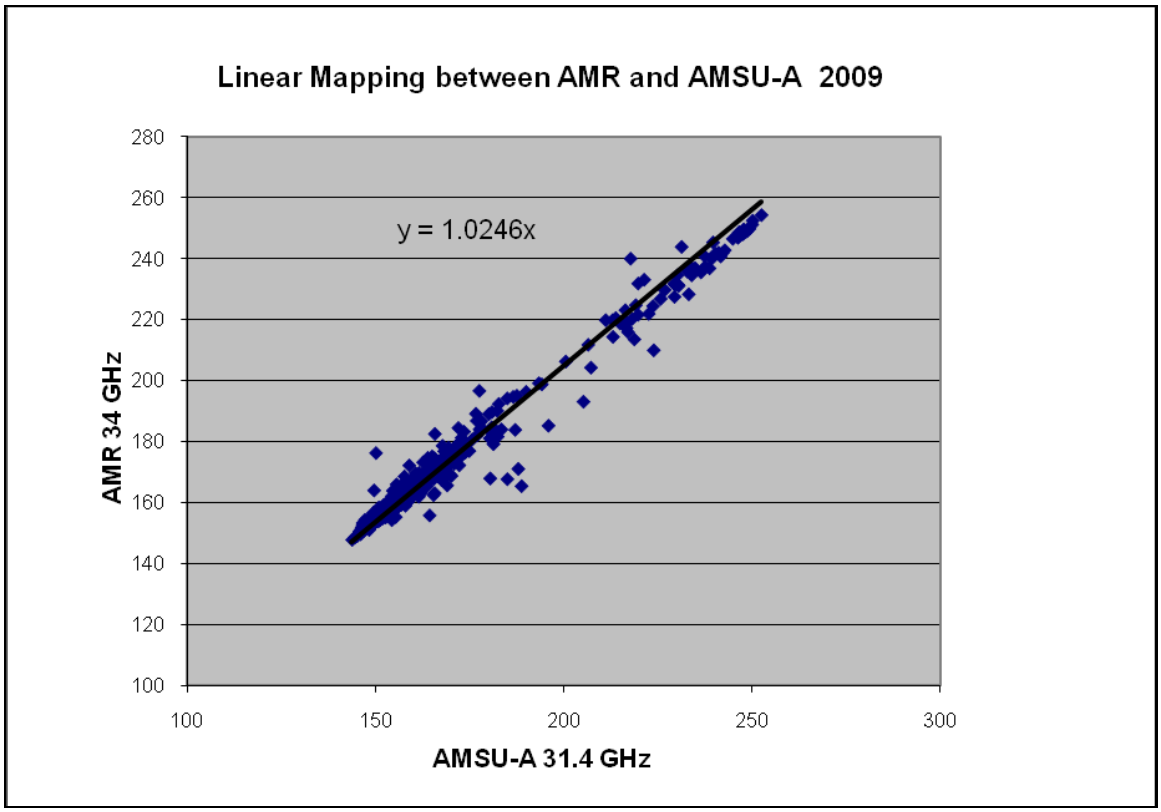
Linear Mapping between AMR and AMSU-A 2009
y = 1.0246x
AMR 34 GHz
AMSU-A 31.4 GHz
280
260
240
220
200
180
160
140
120
100
100
150
200
250
300

## 2.3 AMR Water Vapor and Cloud Liquid Water Retrievals

### 2.3.1 AMSU-A Water Vapor and Cloud Algorithms

Since in microwave frequencies the radiance is linearly proportional to temperatures, the brightness temperatures are preferred in the algorithm. Using Eq. (4) of Weng's 2003 paper, the cloud liquid water and total precipitable water can be derived using two AMSU window channels at 23.8 and 31.4 GHz (Weng et al., 2003) assuming an isothermal atmosphere. Essentially, cloud liquid water ($L$) and total precipitable water ($V$) are derived using

$$L = a_0 \mu \left[ \ln(T_s - TB_{31}) - a_1 \ln(T_s - TB_{23}) - a_2 \right]$$

and

$$V = b_0 \mu \left[ \ln(T_s - TB_{31}) - b_1 \ln(T_s - TB_{23}) - b_2 \right] ,$$

Where $T_s$ is the sea surface temperature, respectively, and the coefficients are defined in Weng et al. (2003) and are functions of ocean surface wind, surface emissivity, and cloud layer temperature if clouds exist in atmosphere.

### 2.3.2 Total Precipitable Water and Cloud Liquid Water Retrievals

AMR swath data which includes brightness temperatures with latitude/longitude information from channels 23.8GHz and 34.0GHz and satellite observation times during the day were extracted from original data set and written into files in ASCII format then converted to grid files in binary format in ascending and descending situations [Figure 1, 2] in order to easily compare to AMSU-A data. Surface winds and sea surface temperatures of the auxiliary data required in above algorithm formula are

taken from Global Data Assimilation System (Gdas) data which is a grid data from 1-360° and 90S-90N with both latitude/longitude resolution at 1 degree. To get the correspondent Gdas data for satellite observation, 4 Gdas files are needed and read simultaneously and interpolated by weight spatially and temporarily according to satellite observation time [Figure 3, 4].

AMR brightness temperatures were substituted into AMSU water vapor and cloud retrieval algorithm equations based on above mapping relation with correspondent auxiliary Gdas sea surface winds and sea surface temperature data to get daily AMR total water vapor and cloud liquid water data for 2008, 2009 [Figure 5, 6]. The monthly averaged TPW and CLW are also computed and plotted [Figure 7, 8].

### 2.4 AMR Algorithm Performance

TPW is very important to short range weather prediction as precipitation, flash flood and other severe weather are closed related to distribution of water vapor. TPW were retrieved over ocean only for this study. Both daily and monthly TPW maps show the large values near tropical region and small values near pole regions which reflect more water vapor with high evaporation, more clouds and precipitations in low latitudes and less water vapor with low evaporation, less clouds and precipitations in high latitudes. The monthly averaged map show that the large TPW values in red move northward slowly while its intensities are getting slightly stronger (red areas becoming larger and brighter) from April to September then move gradually southward with their intensities becoming weaker from October to March. We can monitor the location, extent and movement of tropical

moisture from these movements which is useful for operation forecaster to do severe weather and precipitation forecast [Figure 9 to 20].

The half year and yearly averaged TPW maps [Figure 21-23] look similar to those of monthly average as Jason-2 satellite passes over the same point on the Earth's surface (to within one kilometer) every ten days with along track resolution at 5.8km. The Equatorial cross separation is 315 km with nearest neighboring passes are separated by 1.4 degree at the Equator.

CLW plays an important role in the transport of energy (latent heat) in the earth-atmosphere system. Researcher and operation forecaster can use CLW to access cloud type (convective or stratiform) and access aircraft icing. The relative large values which appear in red on the daily CLW maps show that in the places of low level convergence rising motion leads to condensation and more convective clouds in those areas and blue and green colors show less cloud droplets in the columns from surface to top of the atmosphere in those areas. However, there is no clear pattern in the monthly CLW maps as clouds are naturally spottier and not continuous in the atmosphere and in many places of the world there are no clouds with CLW values at zeros. CLW also valid over ocean with values larger than 0.7mm are not reliable.

It is shown in both monthly mean and daily plots that TPW values are about 100 to 200 times of those of CLW which means that water content in the column of atmosphere from surface to top is in the order of hundred times larger in vapor form than in liquid form.

These results are in good agreements with those from AMSU-A on board NOAA-KLM and AMSU-A on board of EUMETSAT's Met-op. The correlation between AMRus (retrieved with our linear method) and AMSU-A for 08012009 (randomly selected) is at 0.9075 for ascending and 0.9055 for descending in the TPW scattered plot [Figure 24 a,b ] after coastal contamination with islands or/and clouds is screened out. The deviation of TPW from AMRus subtract AMSU-A data is 9.18993mm for ascending case and 8.75910mm for descending case which is good considering many TPW values over 70mm.

TPW and CLW which were retrieved by Centre National d'Etudes Spatiales (CNES) were also extracted from original AMR data set and used to compare to our retrieved TPW and CLW in linear mapping technique with very good agreements: The daily correlations between our retrieved TPW and those of CNES retrieved for 08012009 (randomly selected) are at 0.9751 for ascending and 0.9785 for descending [Figure 25a,b]. The correlations of August of 2009 monthly averaged TPW between our retrievals and theirs are at 0.9815 for ascending and 0.9823 for descending [Figure 26, 27]. However, the correlations will be a bit lower when smaller TPW values are included. The standard deviation of TPW from AMRus subtract AMRec (retrieved from CNES) data is 3.61641mm for descending case and 3.02215mm for ascending which is very good.

The CLW correlation between our AMR daily retrieved and CNES AMR retrieved is at 0.8604 for descending and 0.7773 for ascending [Figure 28a, b] for 08012009 which is better than the CLW correlation between our AMR retrievals to AMSU-A retrievals. The randomly selected CLW correlation values for other days [available per request] are between 0.7773

to 0.8604. Although the CLW correlation is not as good as that of TPW it is still reasonable and realistic considering that CLW is a less continuous and spottier parameter comparing to TPW. The CLW is also evaluated by plotting cloud cover comparison between our linear mapping retrievals to CNES retrievals and our linear mapping retrieval to AMSU retrievals [Figure 29a, b]. The X-axes is the cloud existence threshold from 0 to maximum CLW here at 2.5 mm. The Y-axes is the percentage of points where both retrievals are higher than the threshold with respect to all retrieved points. It is found between 0.01mm to 0.2mm thresholds both retrievals have the high consistence in cloud existence for both AMRus vs. AMRec and AMRus vs. AMSU-A cases.

All the above results show that the AMR linear mapping technique under SNO condition is a simple but accurate, very efficient and practical retrieval algorithm which can be easily adapted for use in other microwave application of CLW and TPW retrievals for different environments.

## 3. Plan for FY2010 Major Milestones

All of 2009, 2008 daily, monthly mean and yearly averaged maps have been moved to corresponding directories of our web server at /net/www/www/smcd/spb/wyu/AMR for On-line access of AMR TPW and CLW products. It will become available as soon as web master got the time to set up.

## References

Weng, F., L. Zhao, R. Ferraro, G. Poe, X. Li, and N. Grody, 2003: Advanced Microwave Sounding Unit Cloud and Precipitation Algorithms. *Radio Sci.*, **38**, 8,086-8,096.

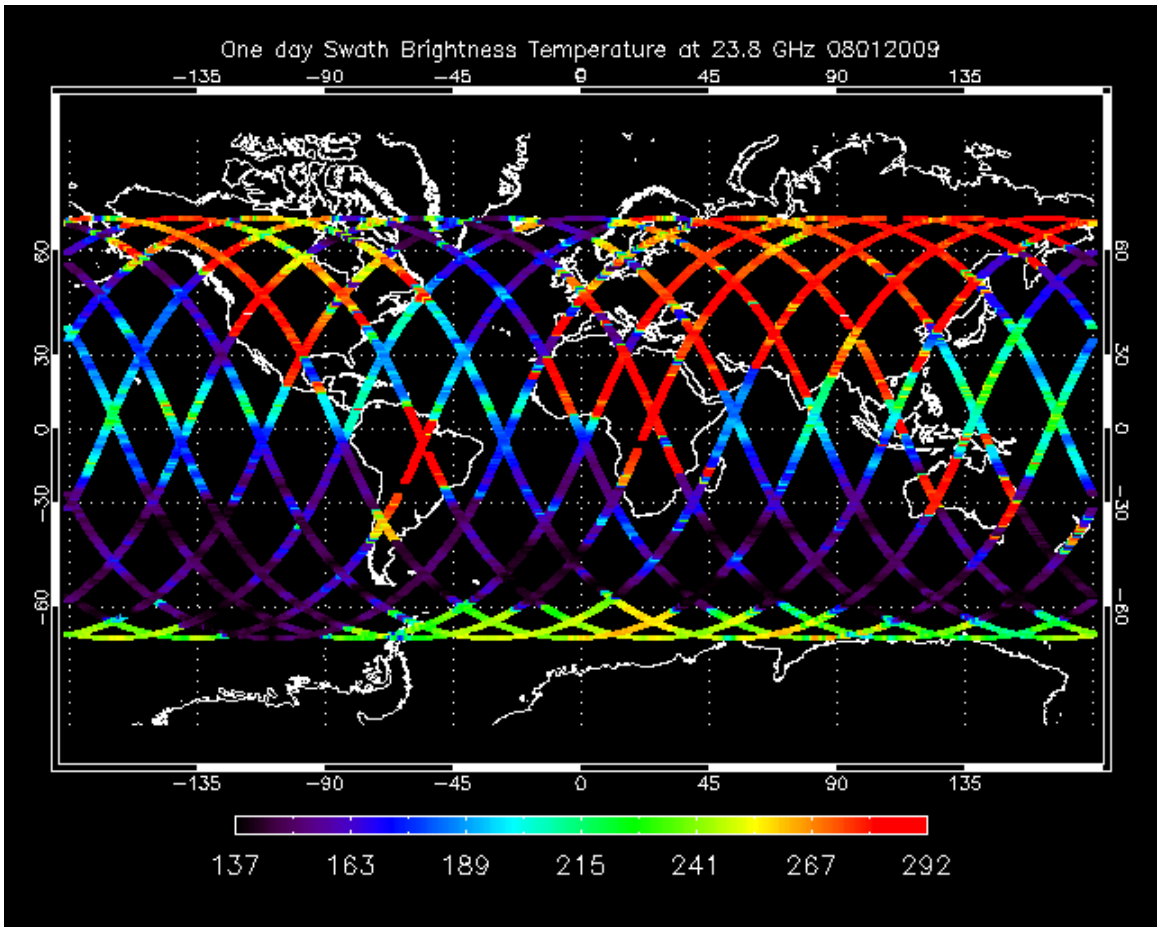


**Figure 1 Swath Tb 08012009**

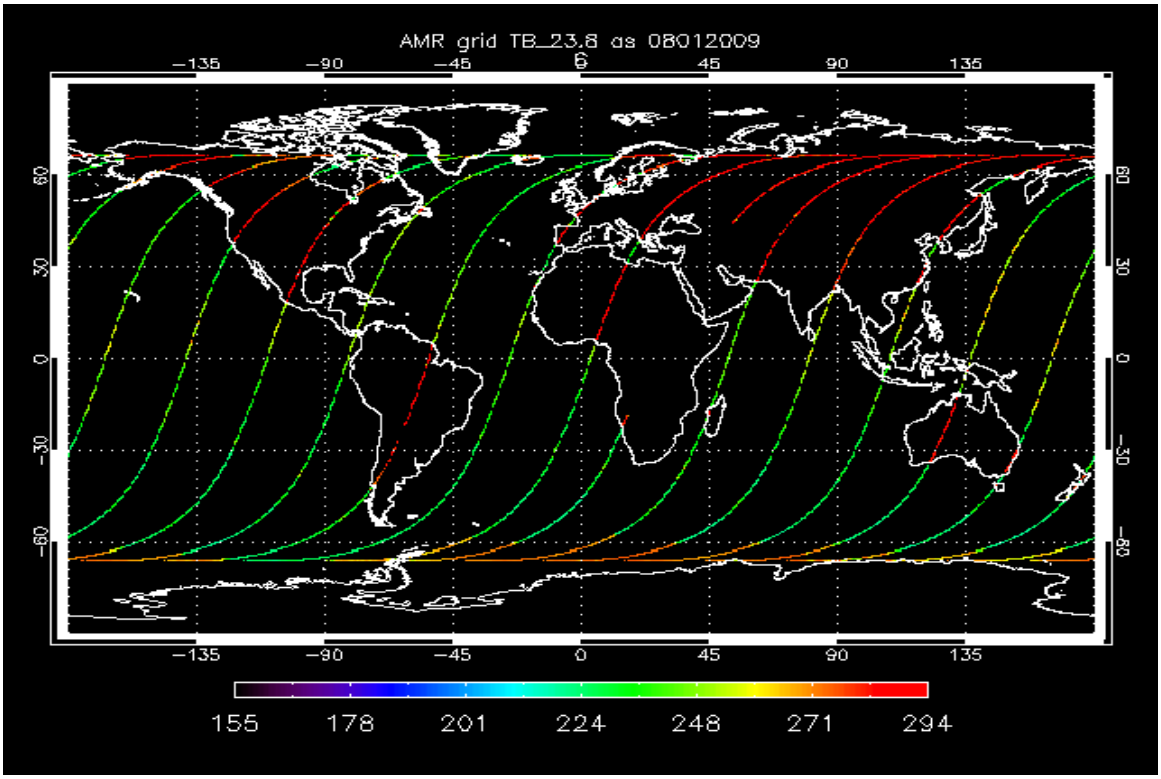


**Figure 2a Grid Tb Asc 08012008**

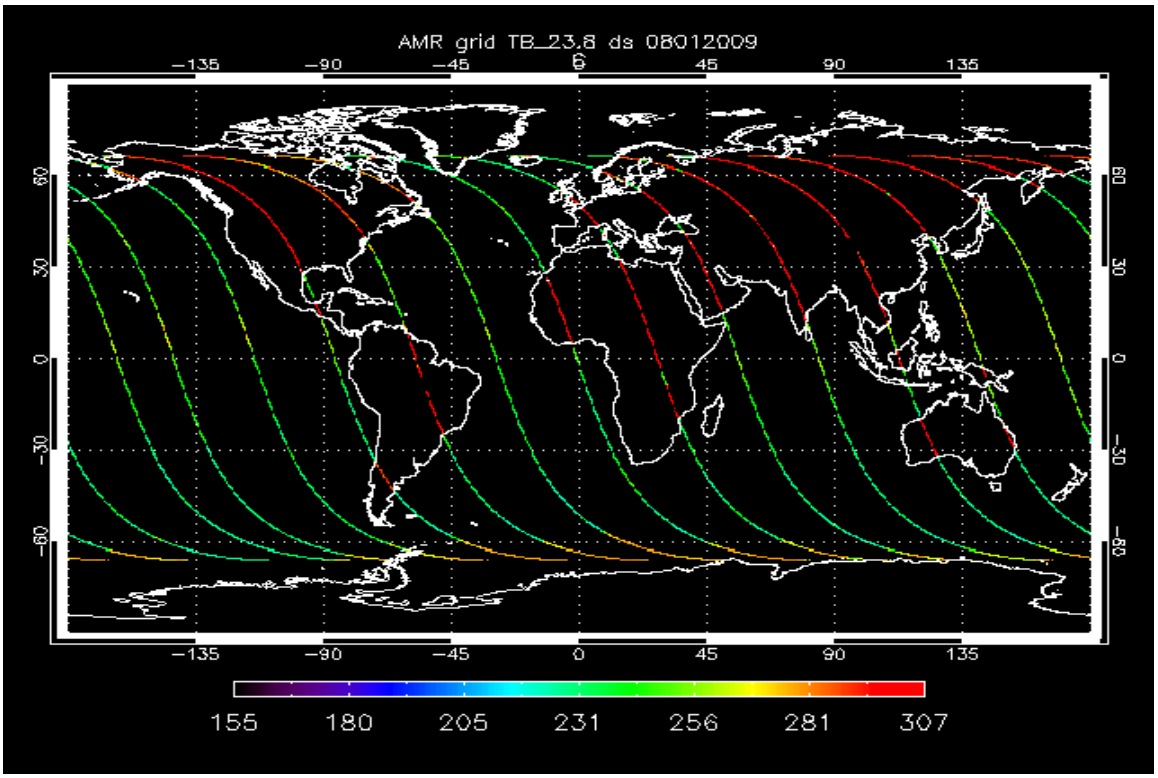


**Figure 2b Grid Tb Dsc 08012009**

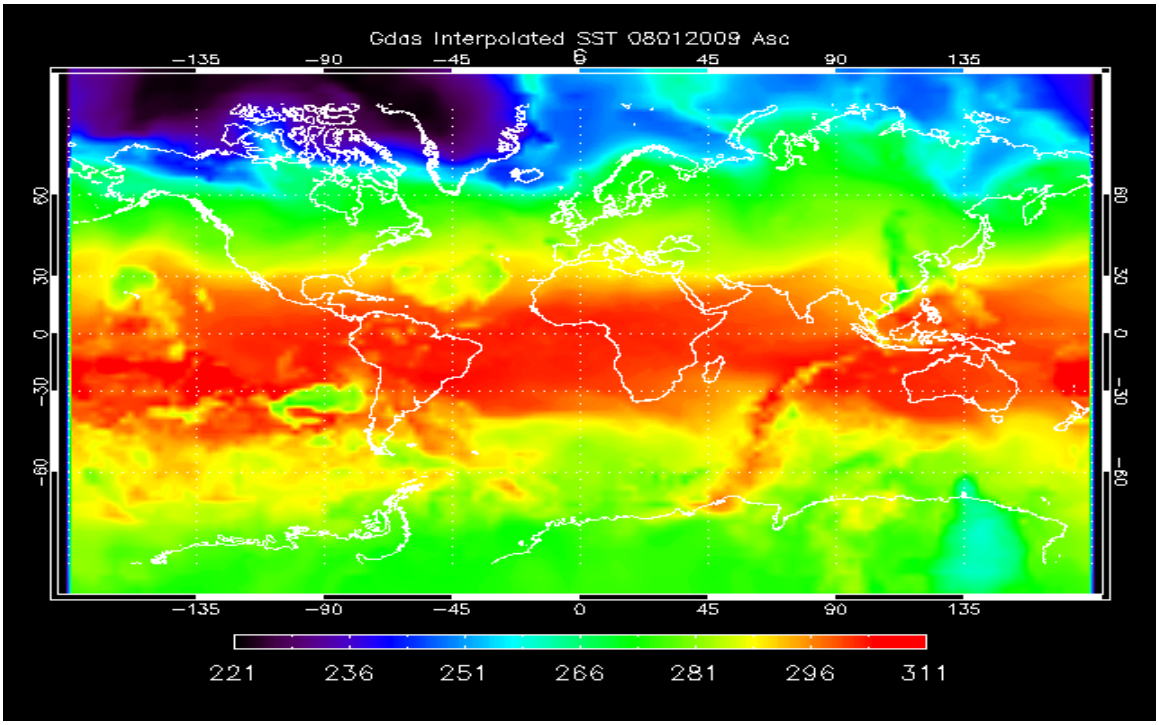


**Figure 3 Gdas Sea Surface Temperatures 08012009**

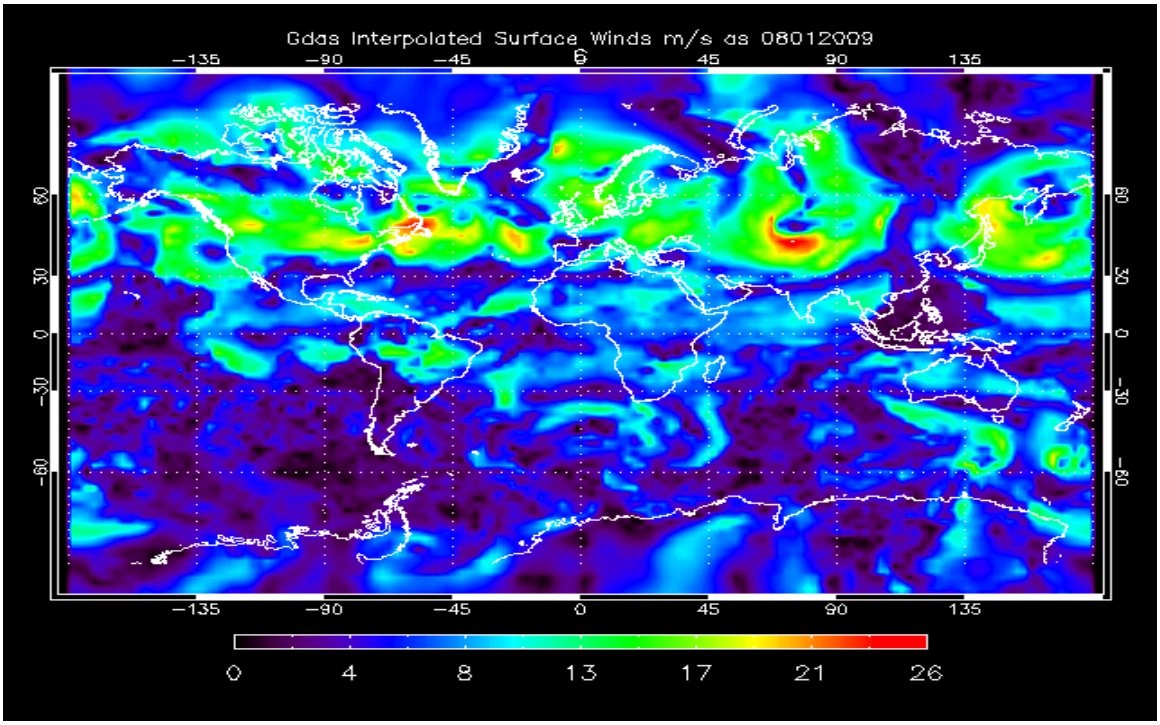


**Figure 4 Gdas Surface Winds 08012009**

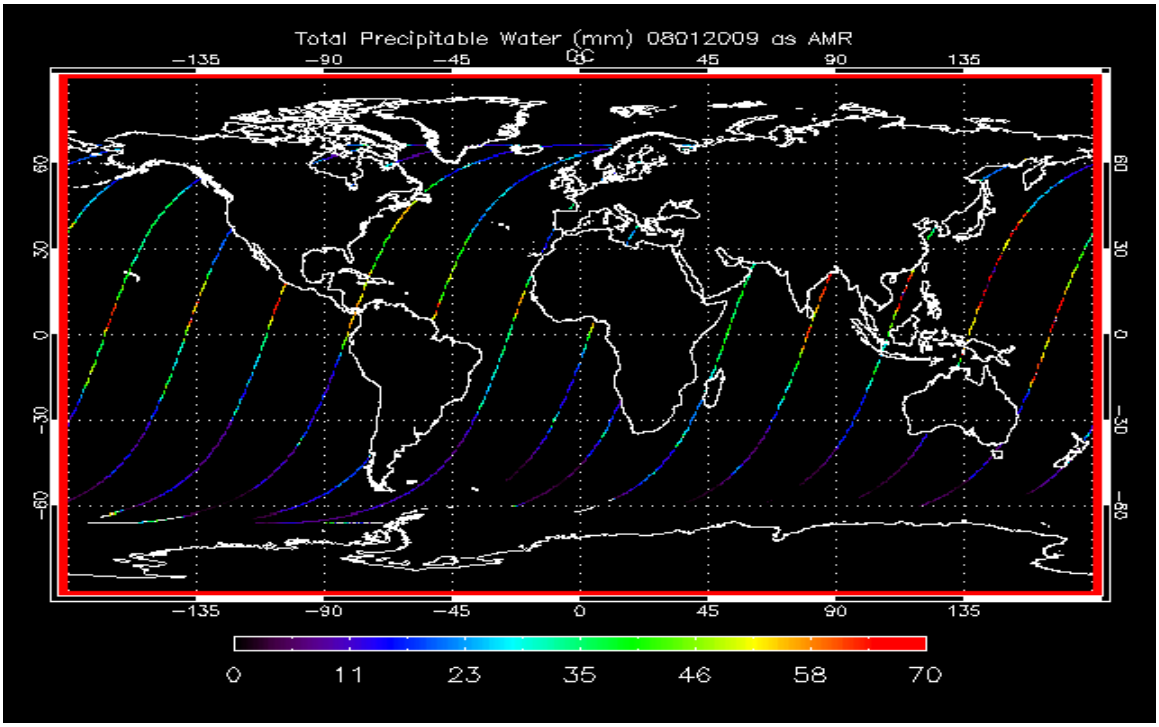


**Figure 5a Daily TPW Asc 08012009**

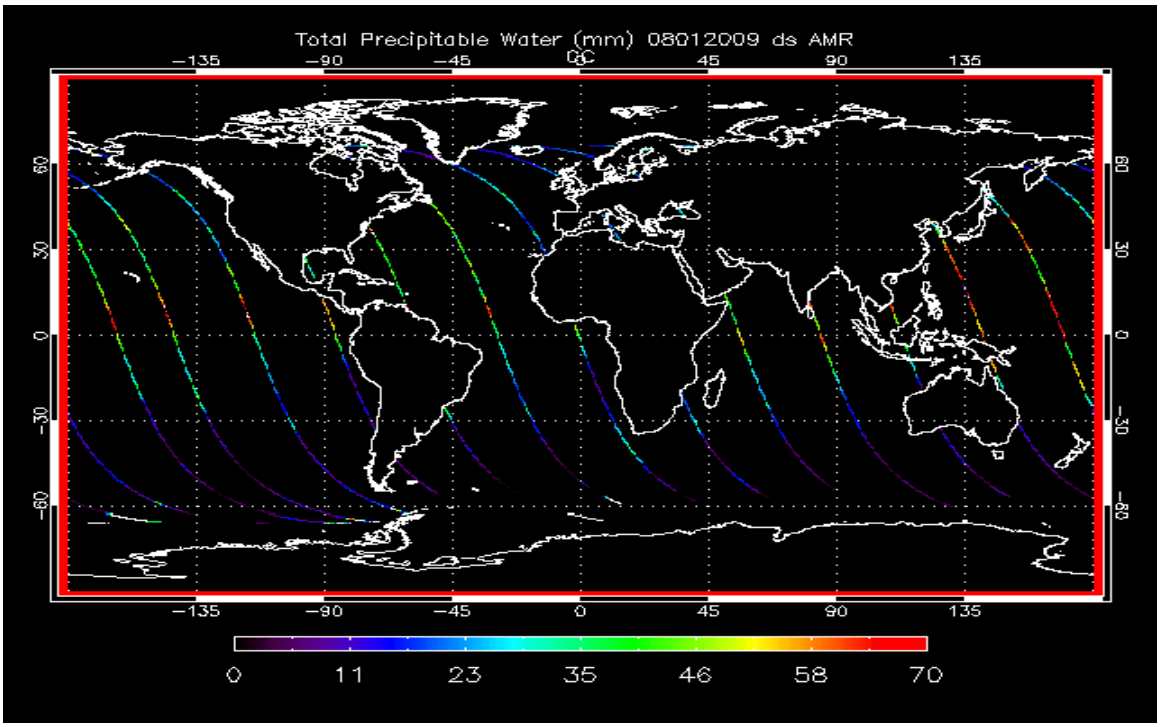


**Figure 5b Daily TPW Dsc 08012009**

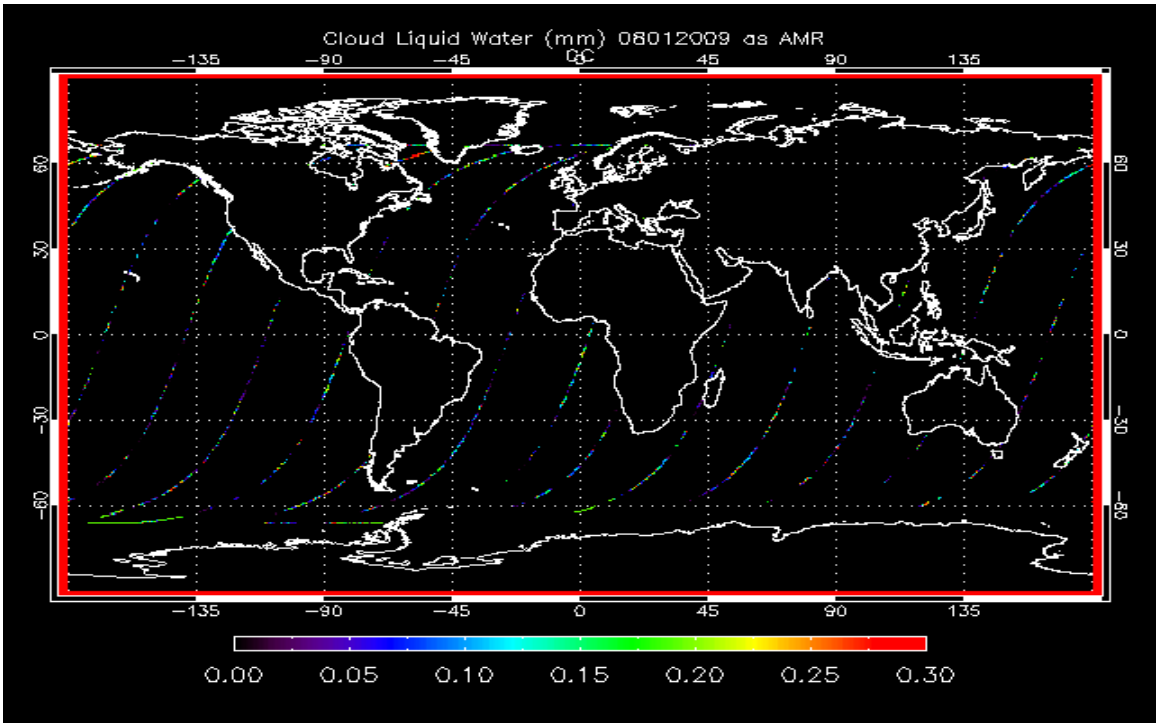


**Figure 6a Daily CLW Asc 08012009**

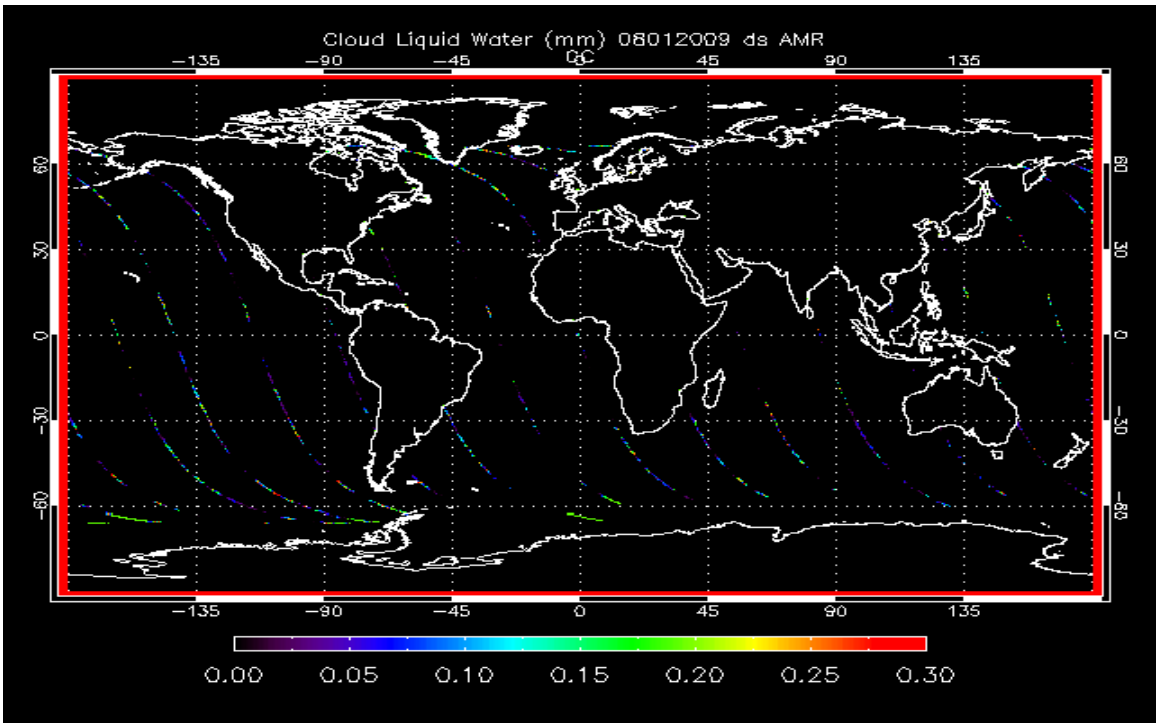


**Figure 6b Daily CLW Dsc 08012009**

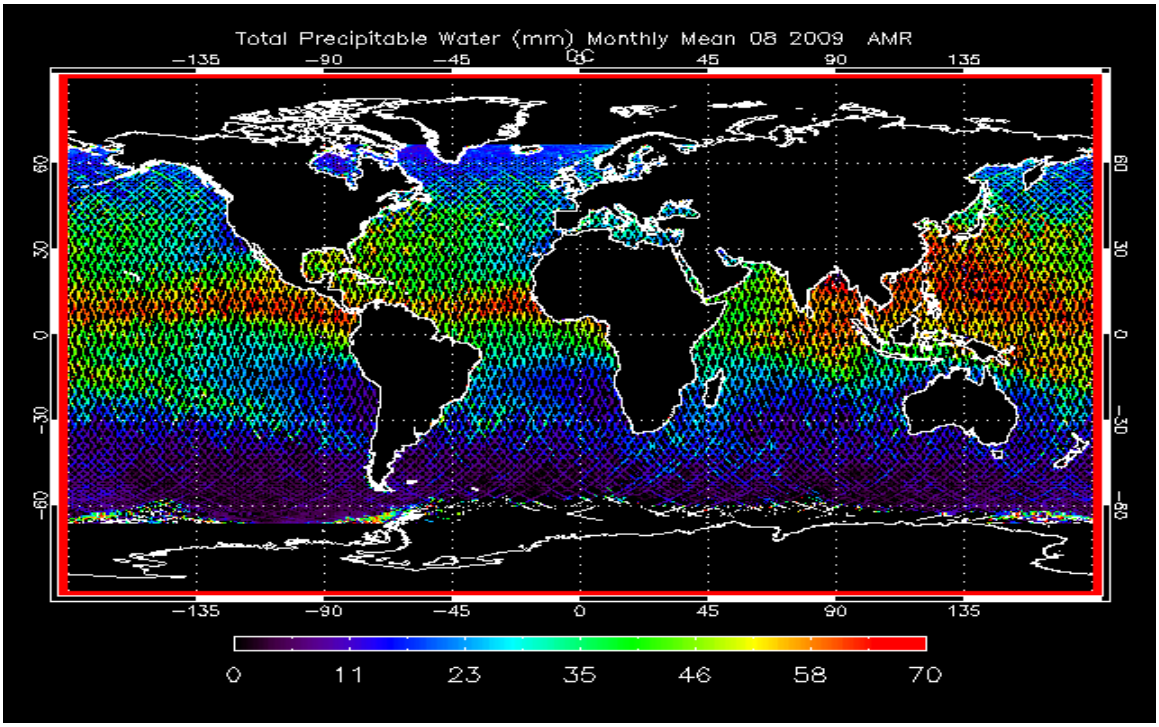


**Figure 7 Monthly Mean TPW Aug. 2009**

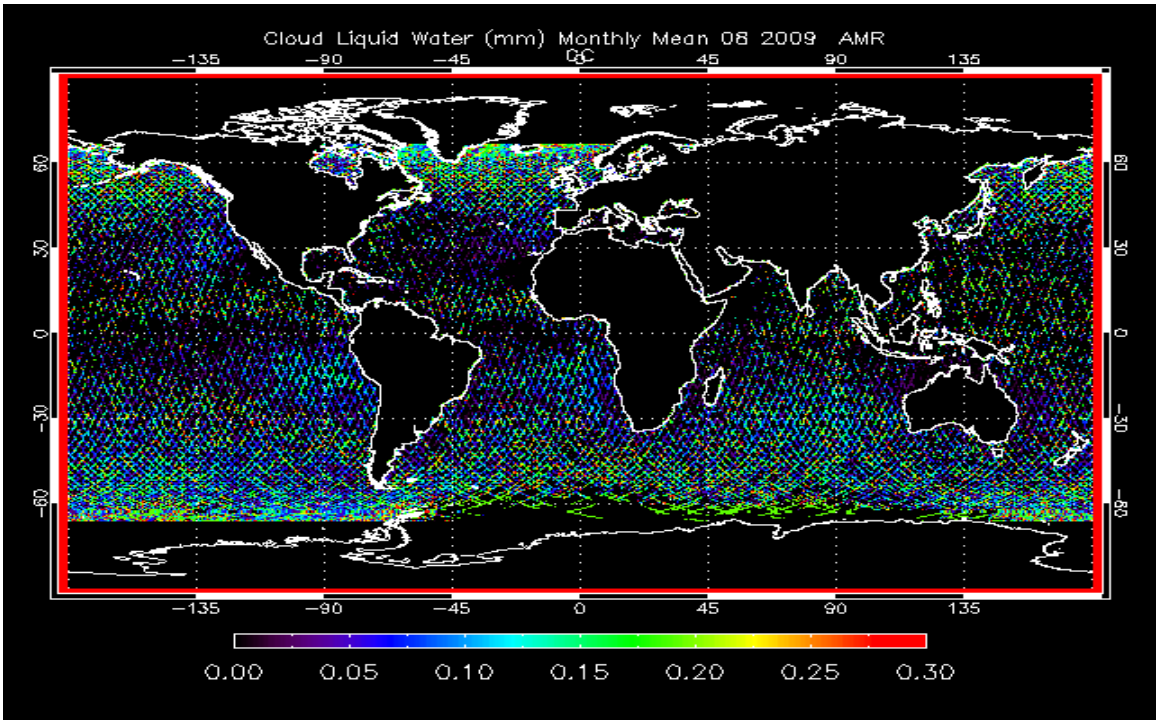


**Figure 8 Monthly Mean CLW Aug. 2009**

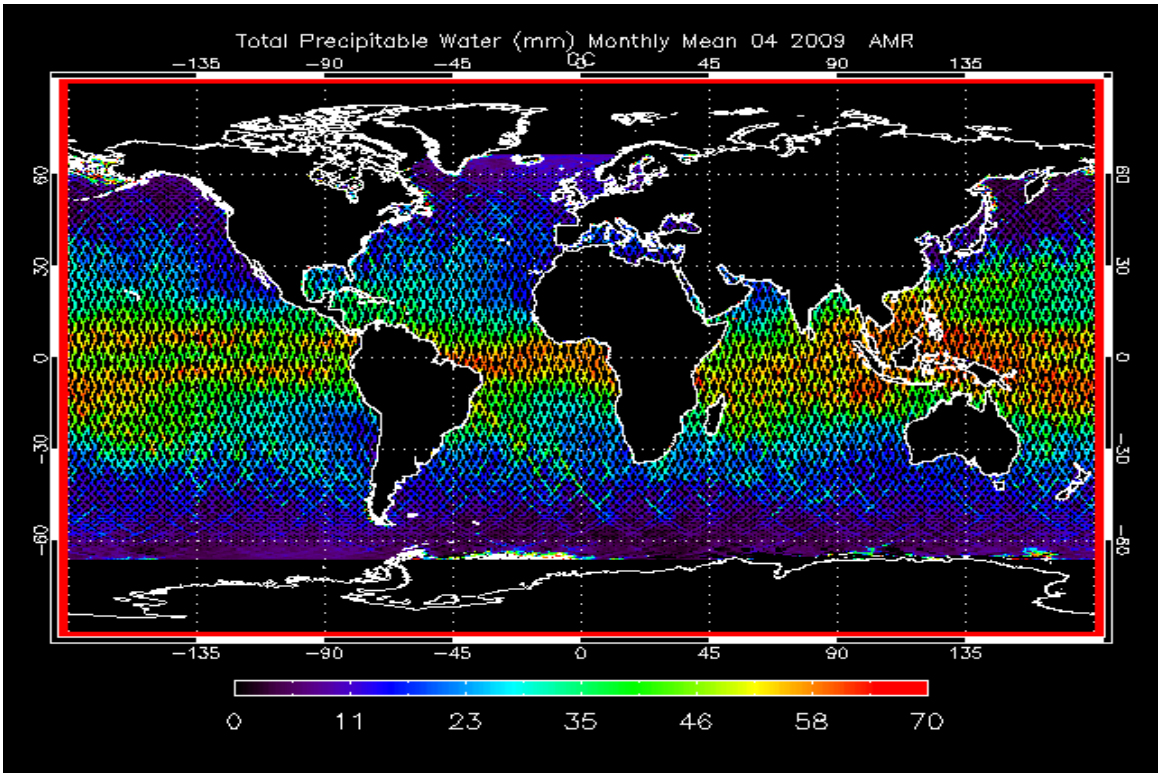


**Figure 9 TPW Monthly Mean April 2009**

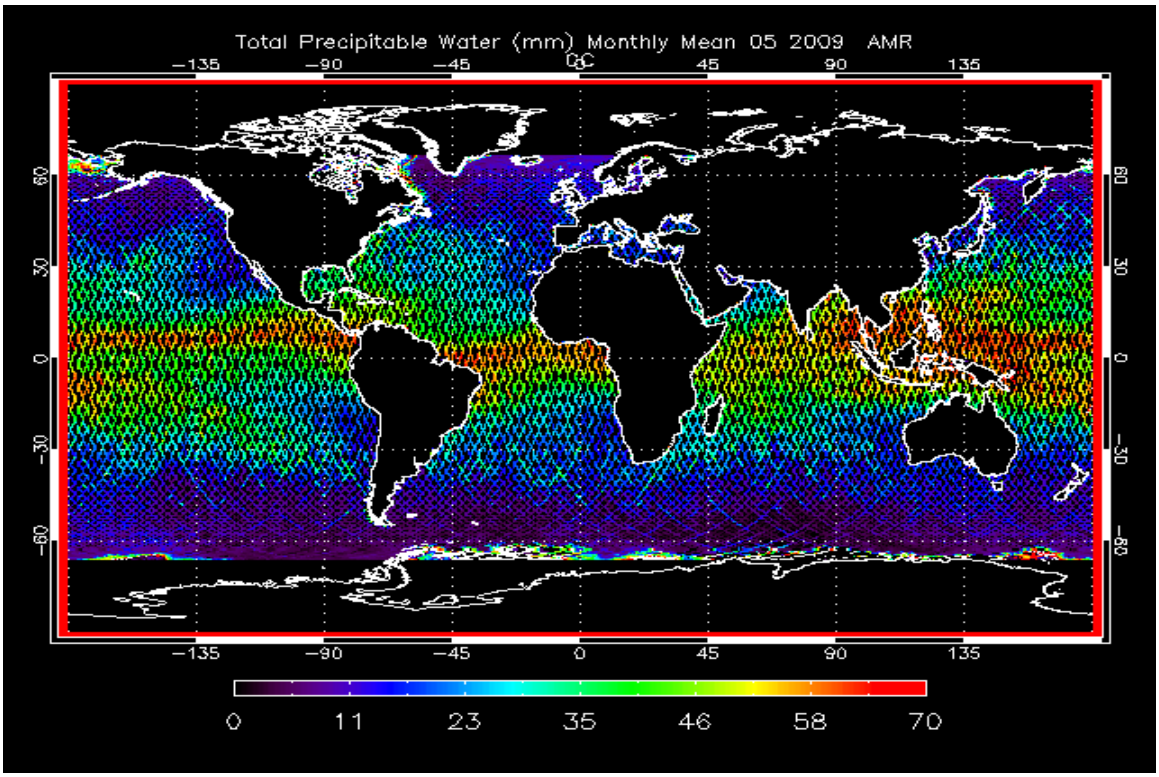


**Figure 10 TPW Monthly Mean May 2009**

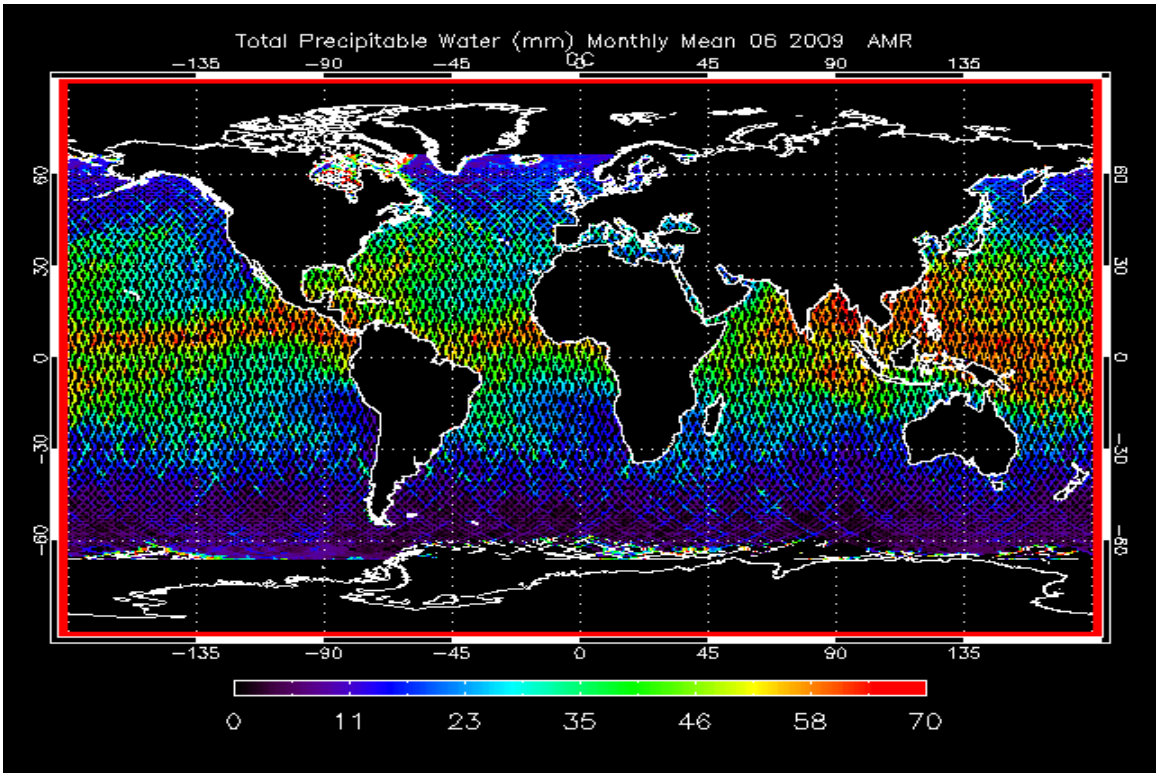


**Figure 11 TPW Monthly Mean June 2009**

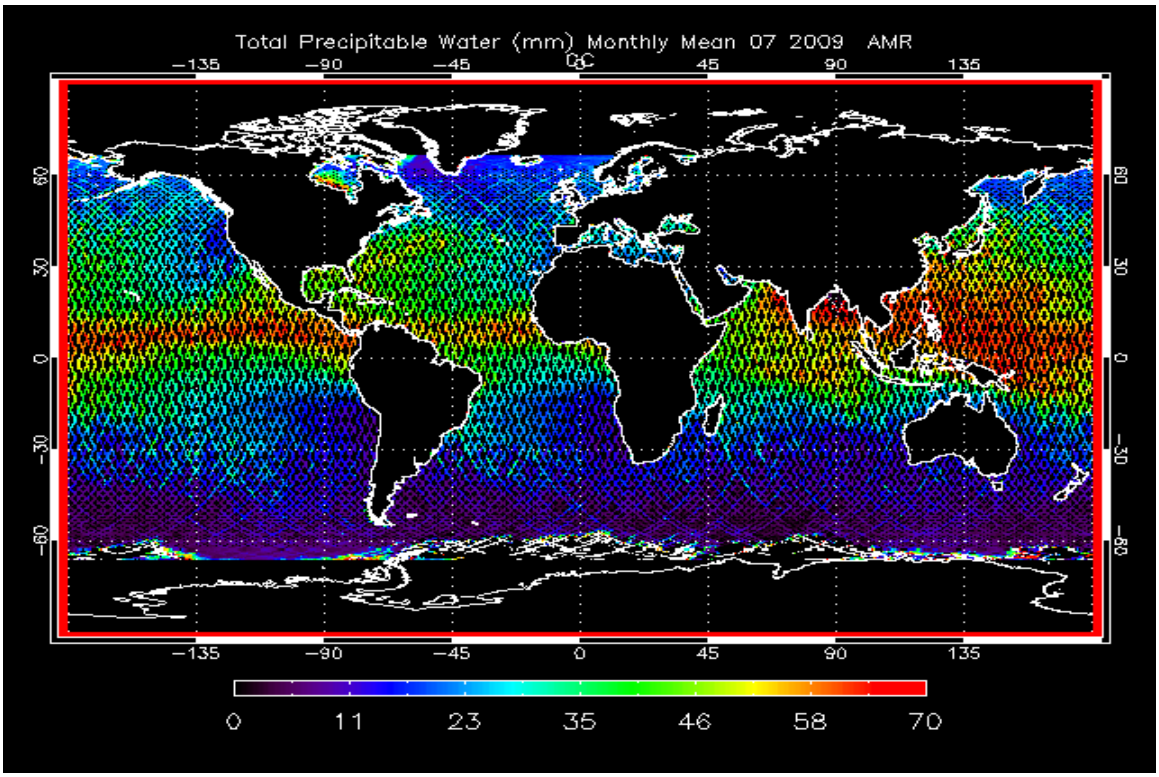


**Figure 12 TPW Monthly Mean July 2009**

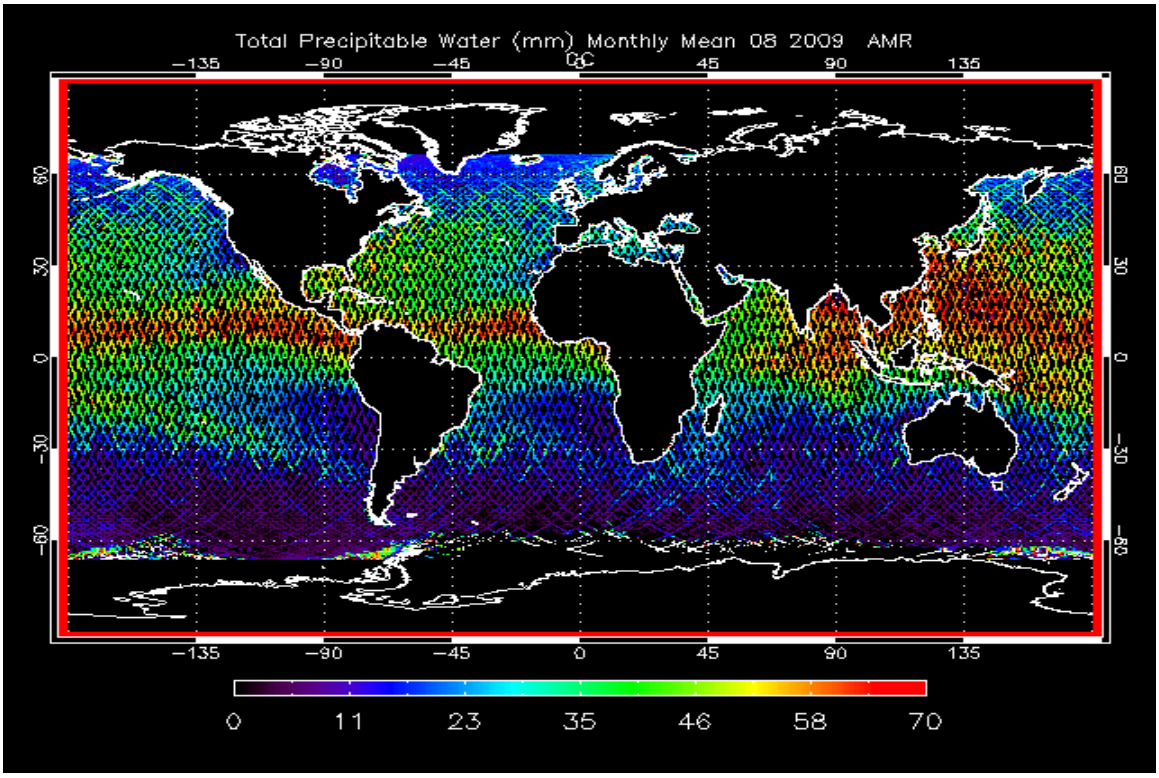


**Figure 13 TPW Monthly Mean August 2009**

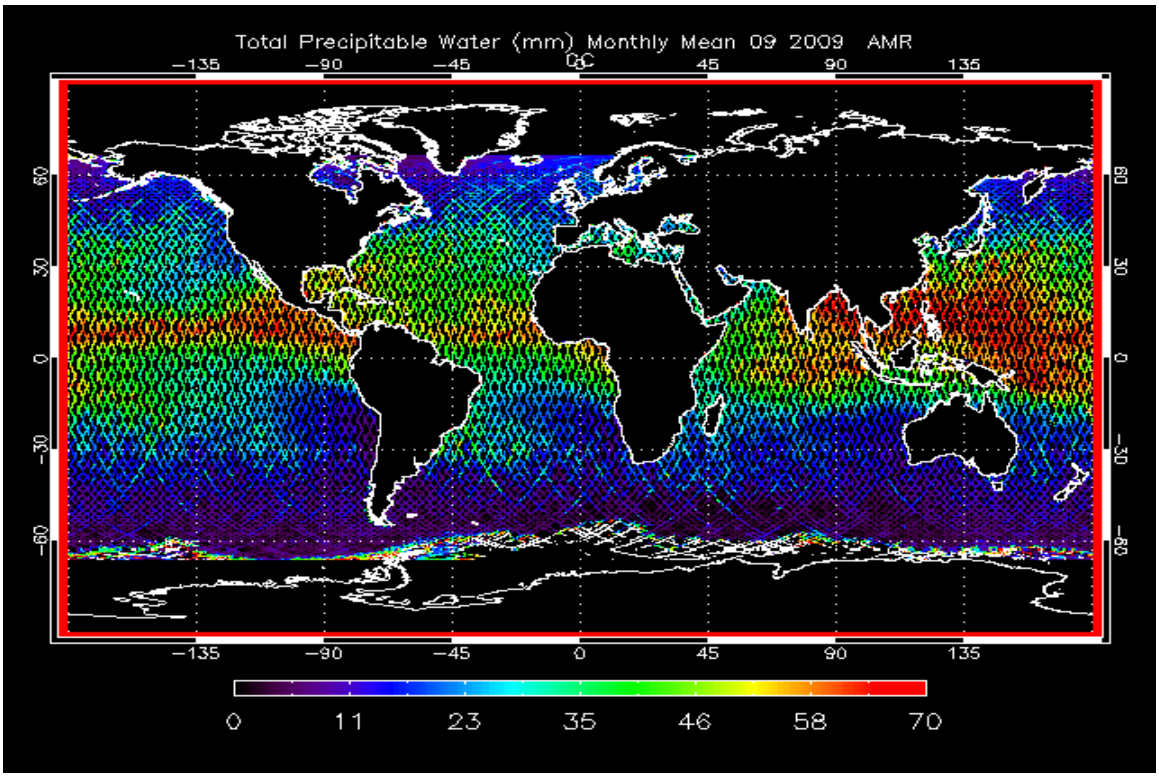


**Figure 14 TPW Monthly Mean September 2009**

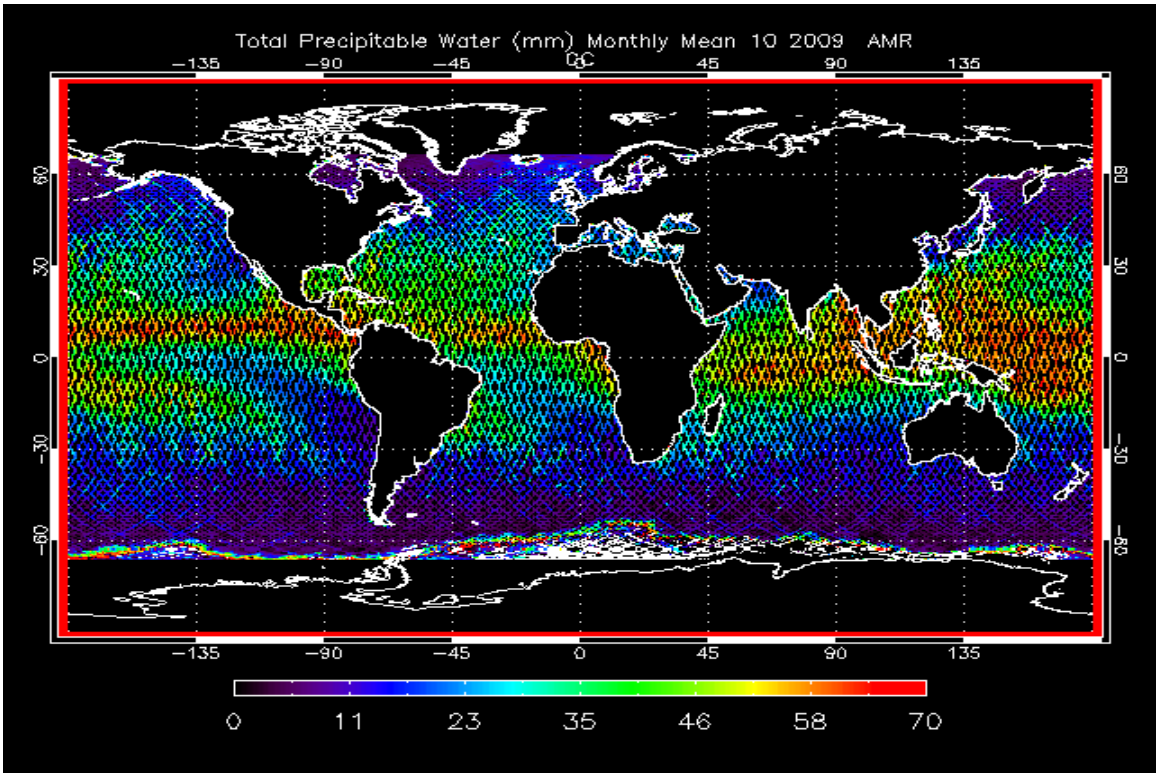


**Figure 15 TPW Monthly Mean October 2009**

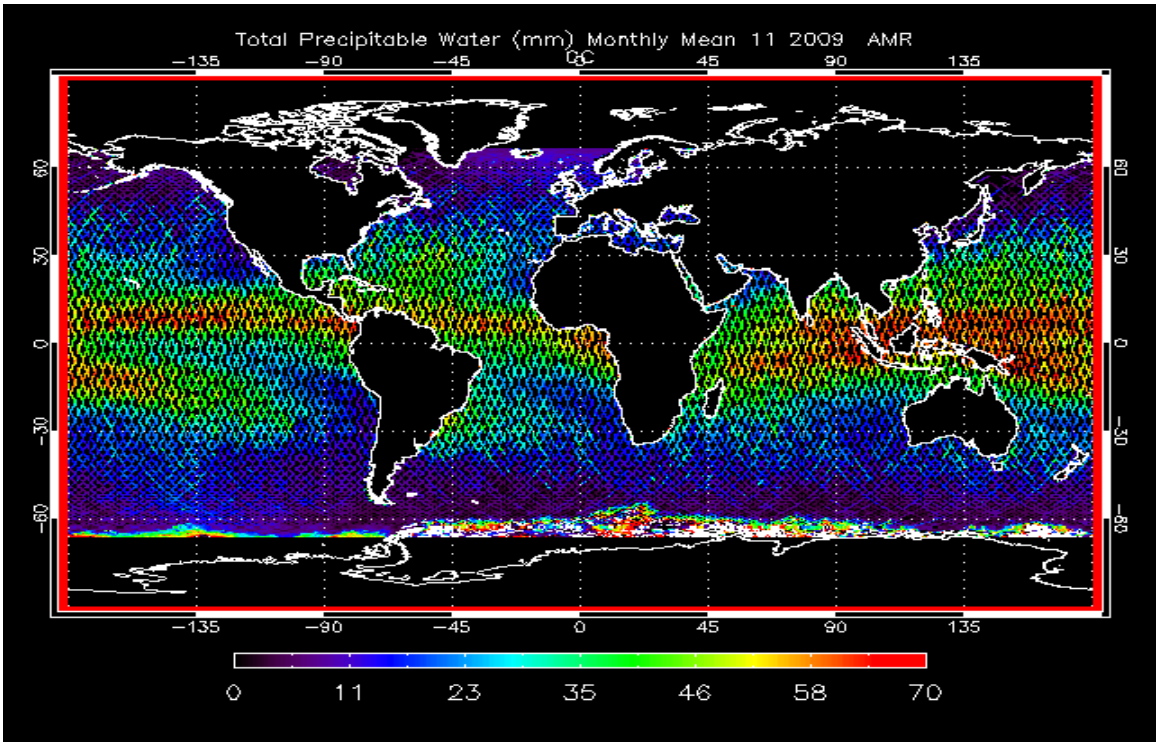


**Figure 16 TPW Monthly Mean November 2009**

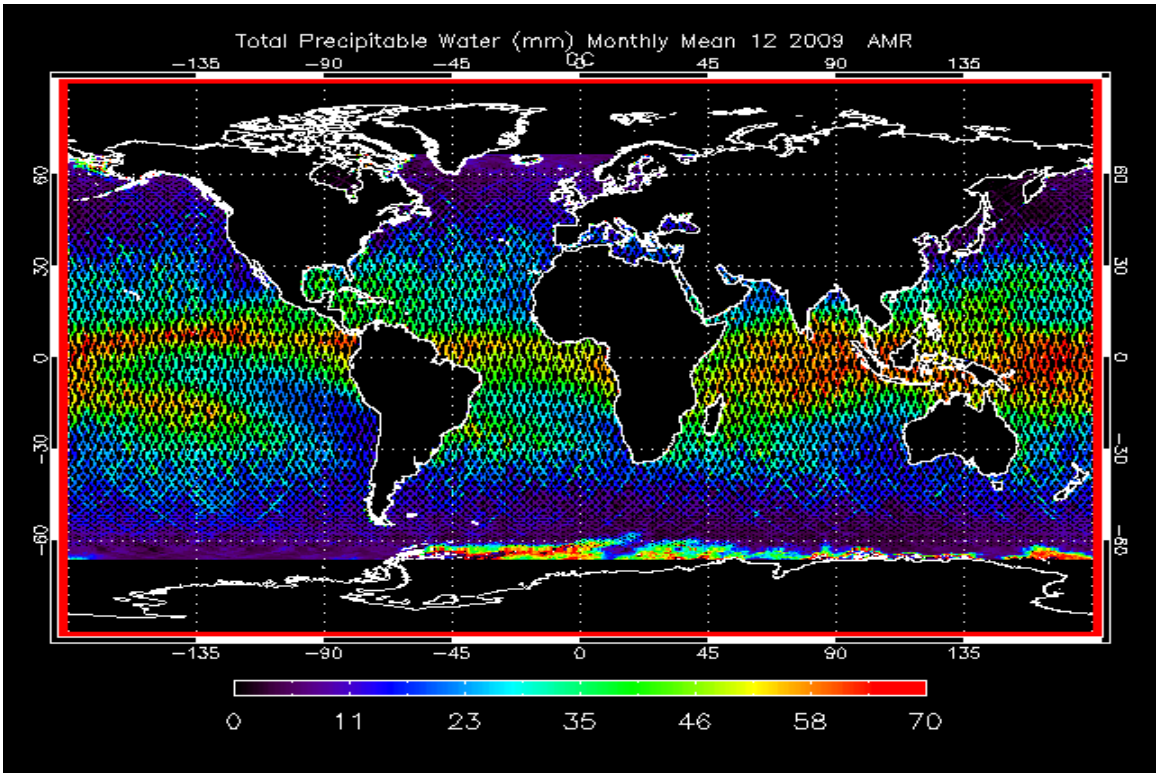


**Figure 17 TPW Monthly Mean December 2009**

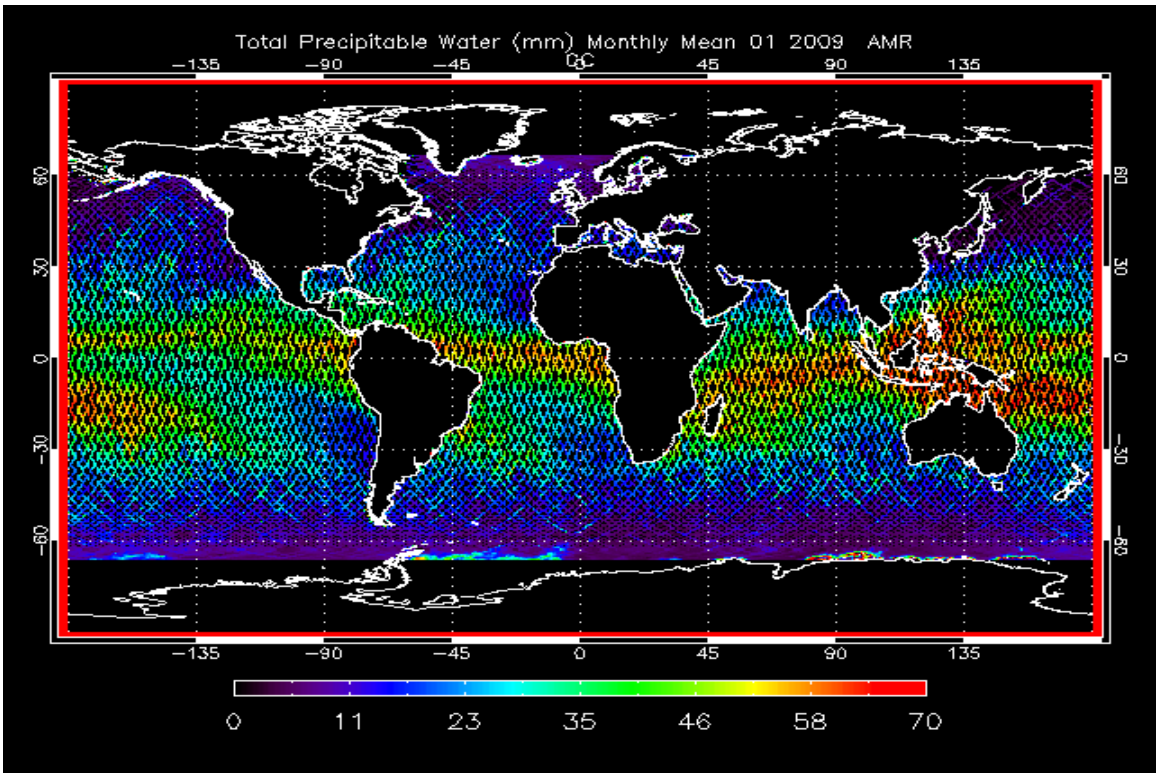


**Figure 18 TPW Monthly Mean January 2009**

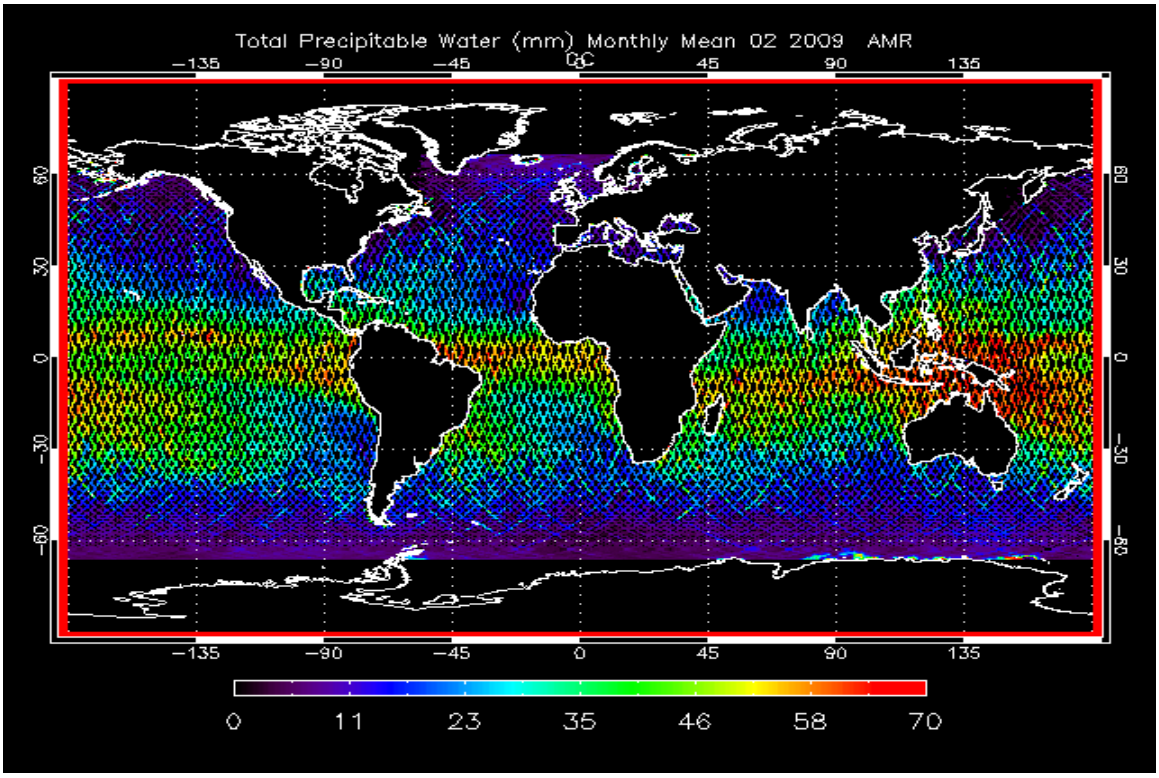


**Figure 19 TPW Monthly Mean February 2009**

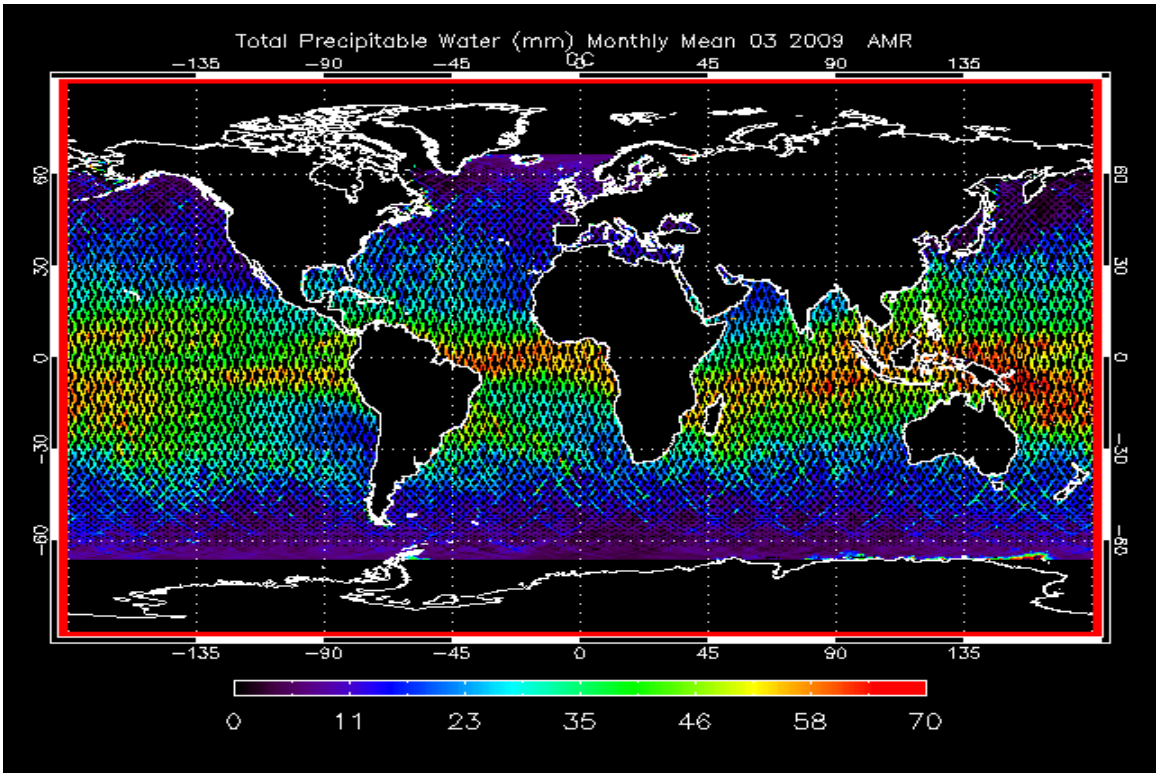


**Figure 20 TPW Monthly Mean March 2009**

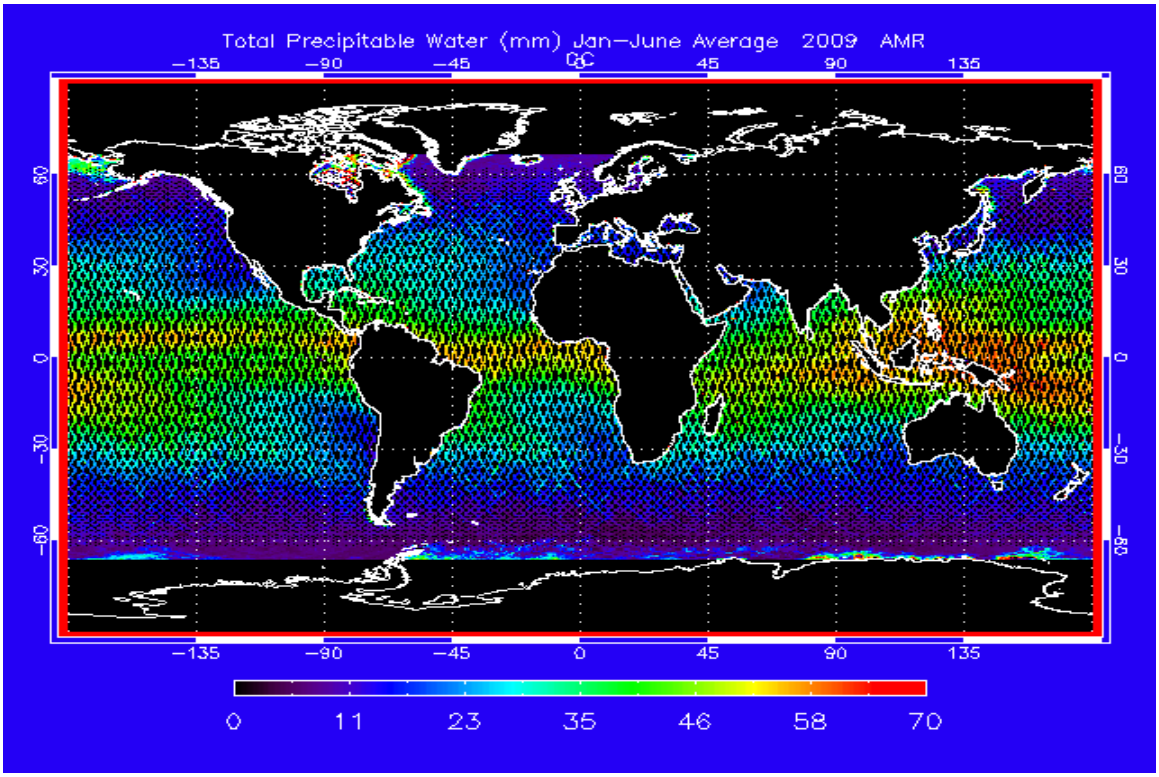


**Figure 21 TPW January-June Average 2009**

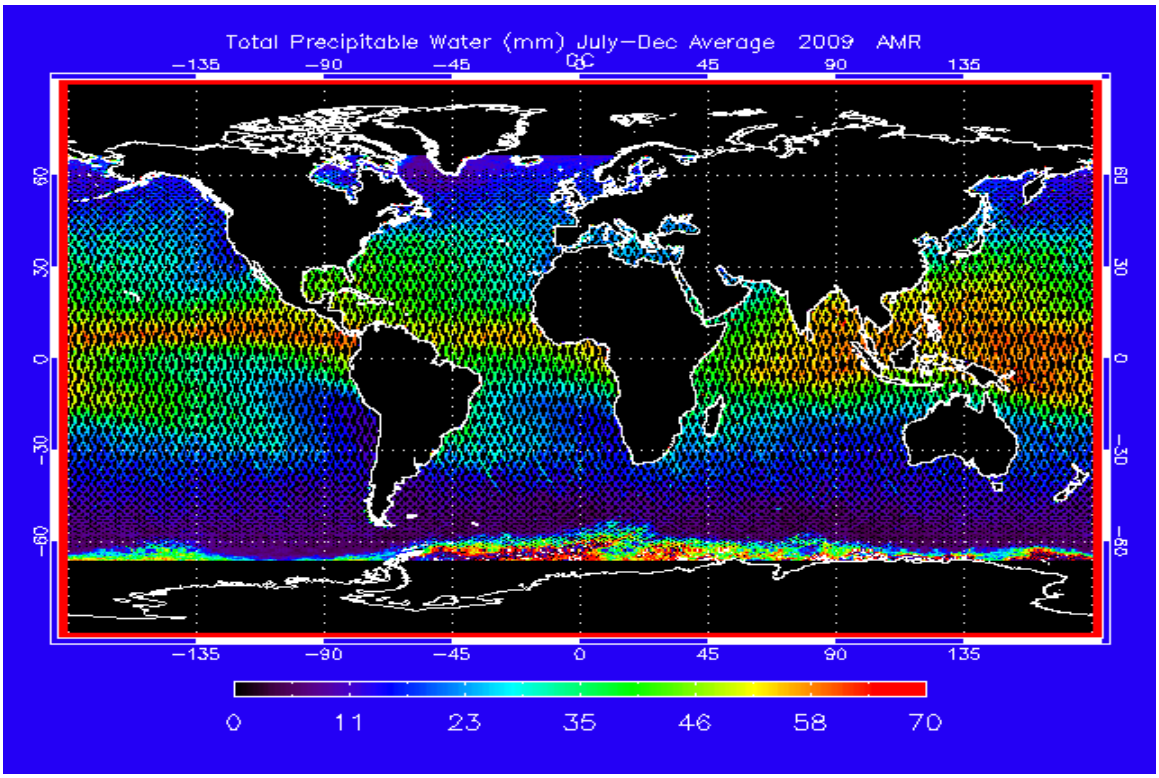


**Figure 22 TPW July-December Average 2009**

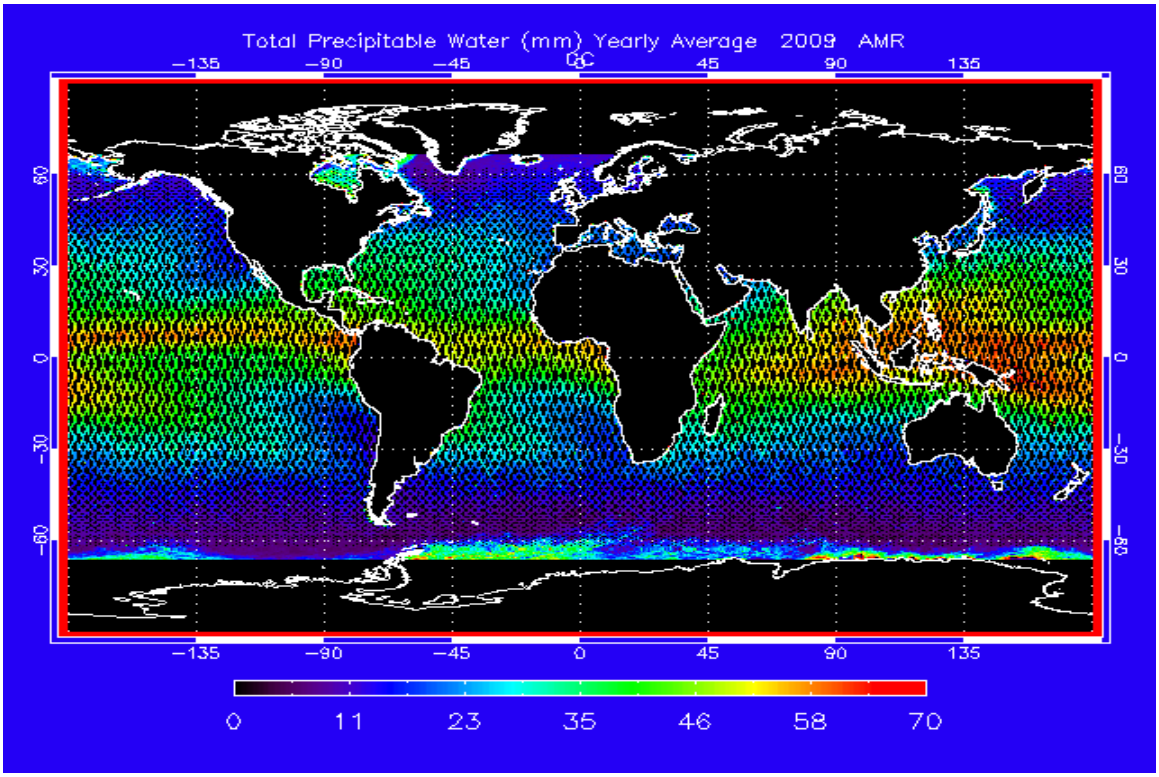


**Figure 23 TPW Yearly Average 2009**

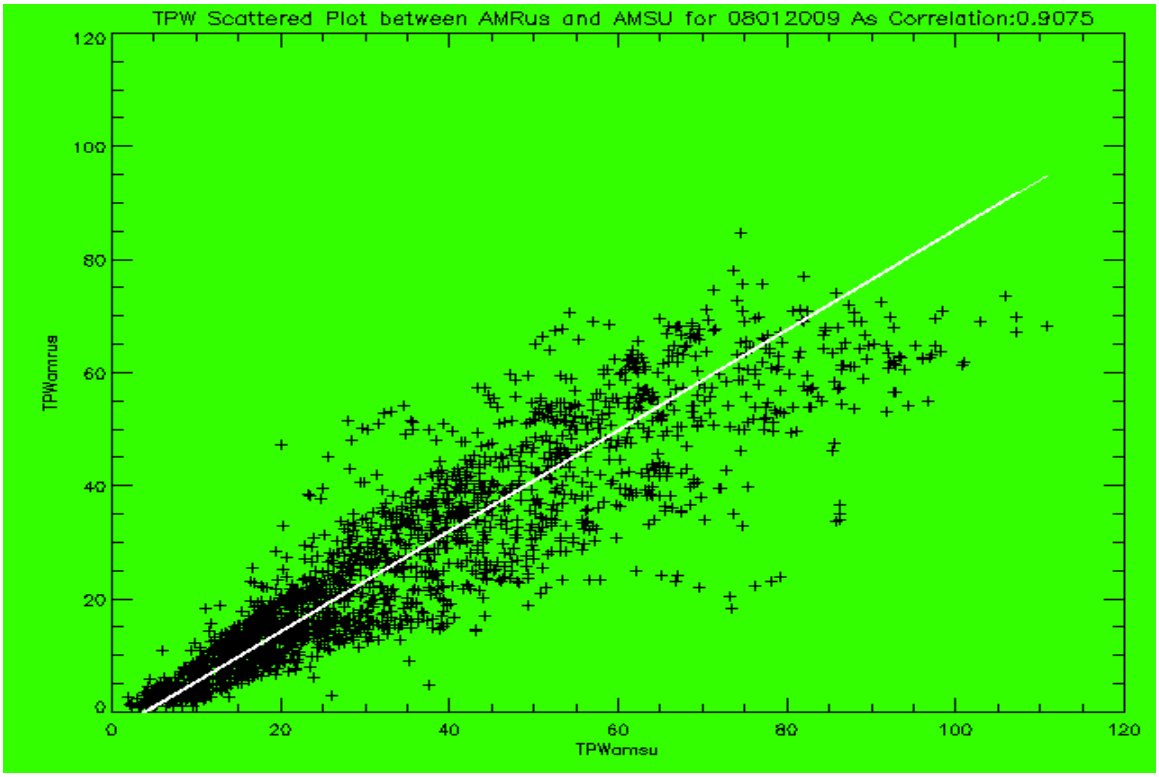


**Figure24a TPW Correlation between AMRus and AMSU-A Asc 08012009**

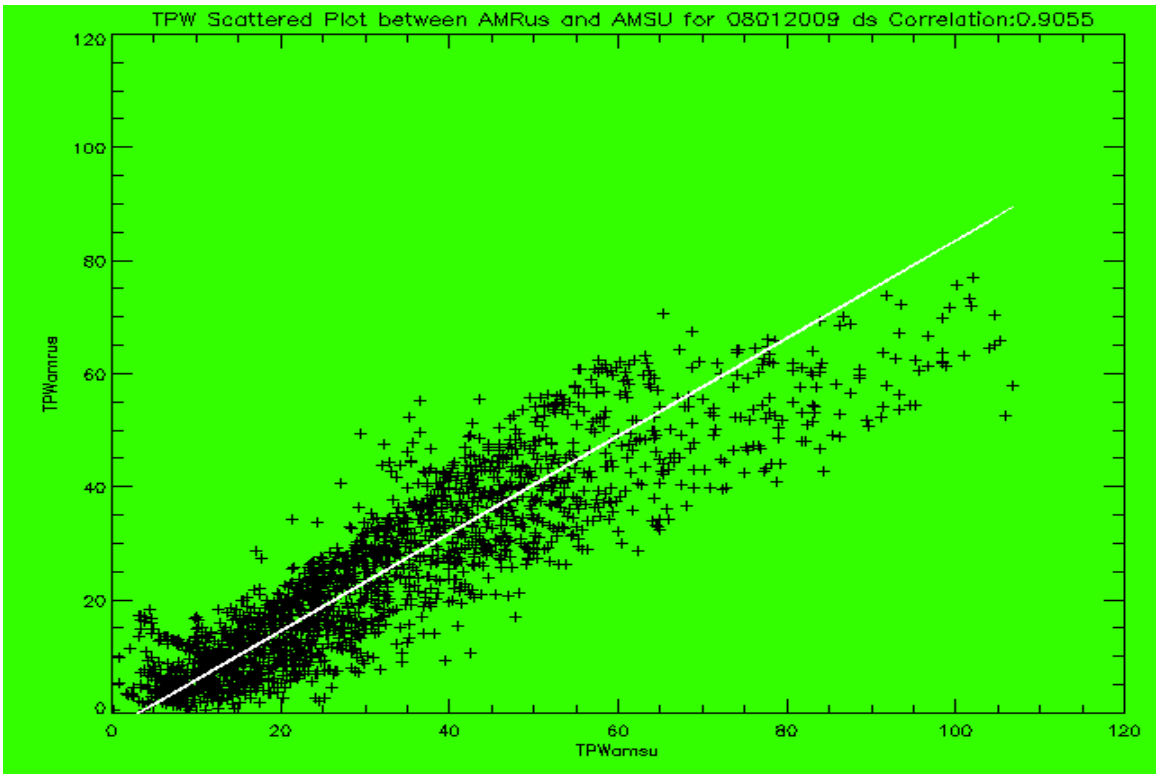


**Figure24b TPW Correlation between AMRus and AMSU-A Des 08012009**

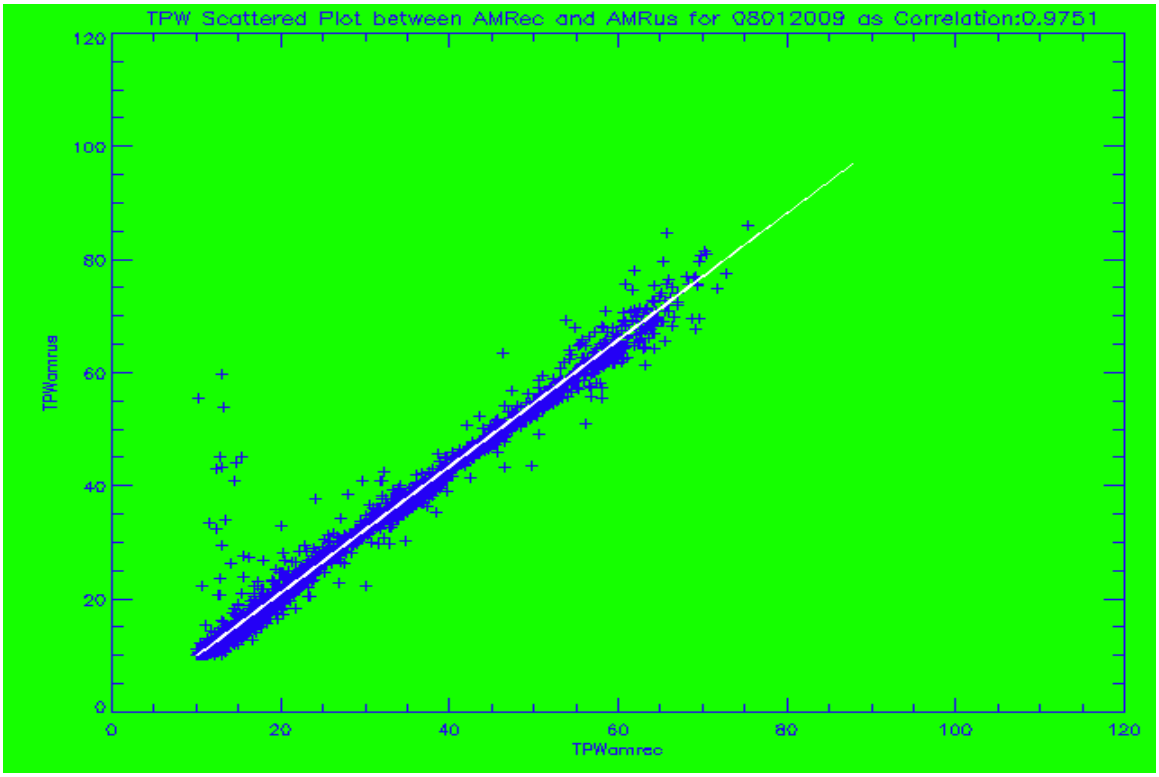


**Figure 25a Daily TPW Correlation between AMRus and AMRec Asc 08012009**

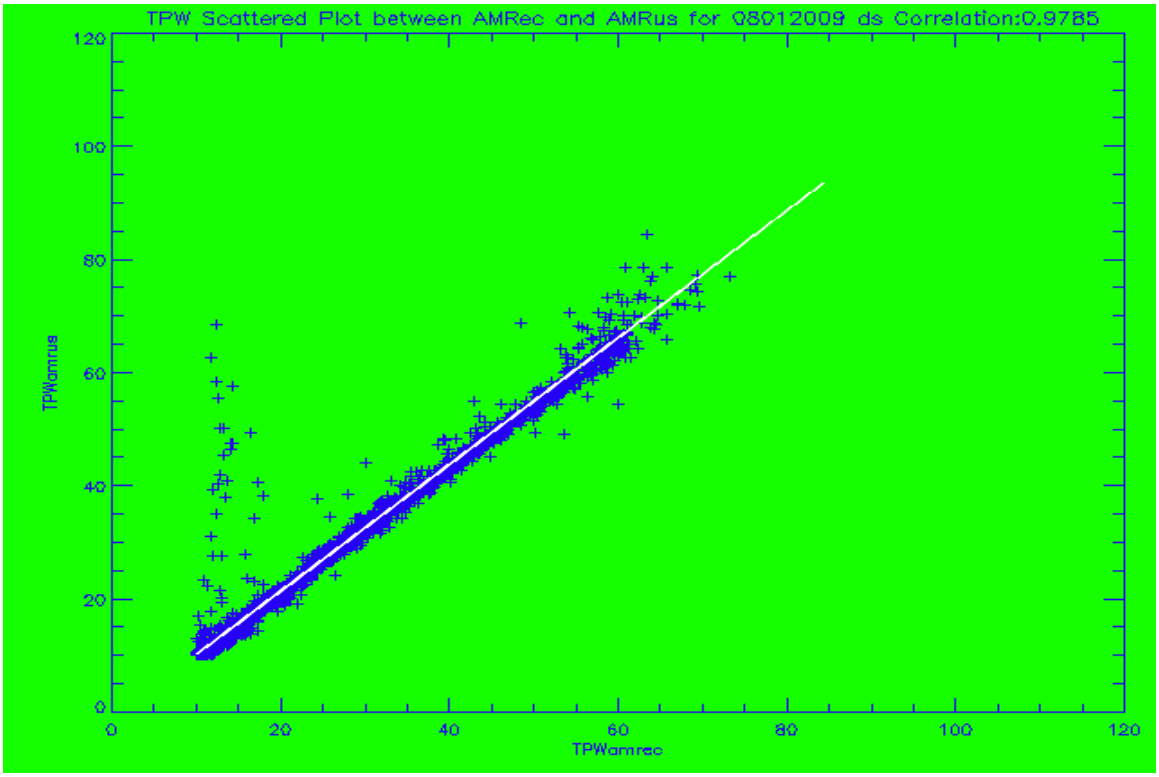


**Figure 25b Daily TPW Correlation between AMRus and AMRec Dsc 08012009**

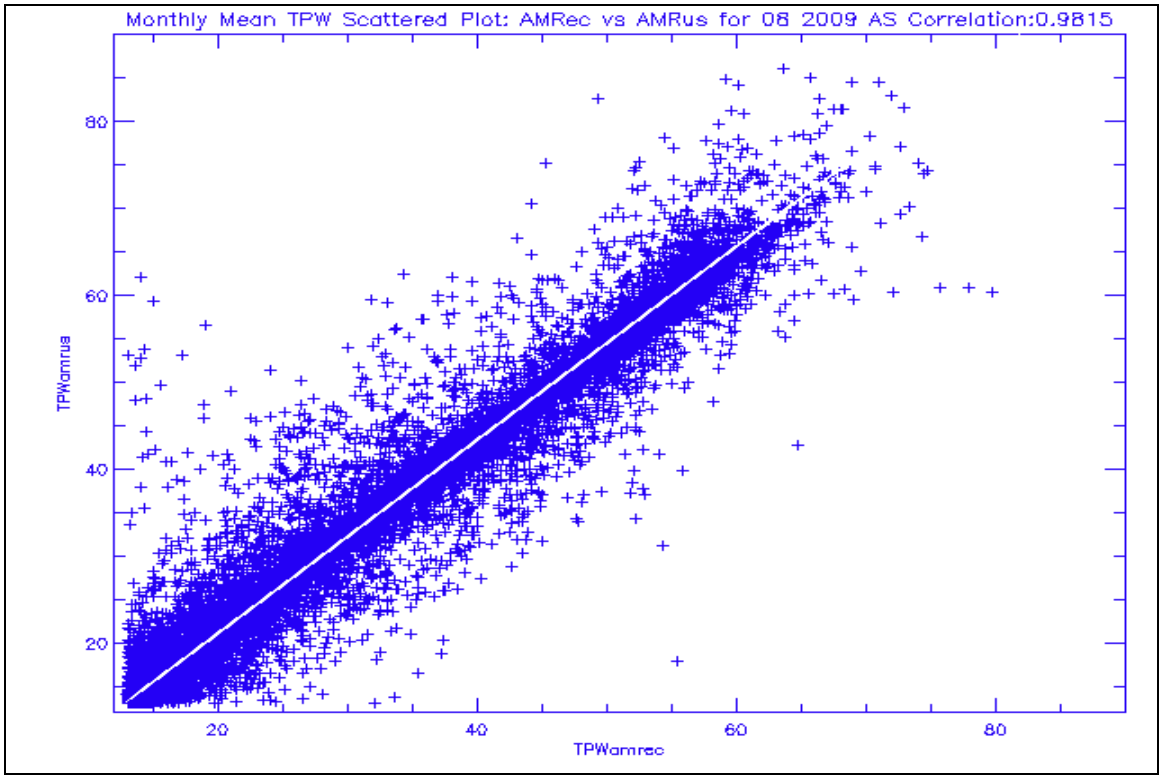


**Figure 26 Monthly TPW Correlation between AMRus and AMRec Asc August 2009**

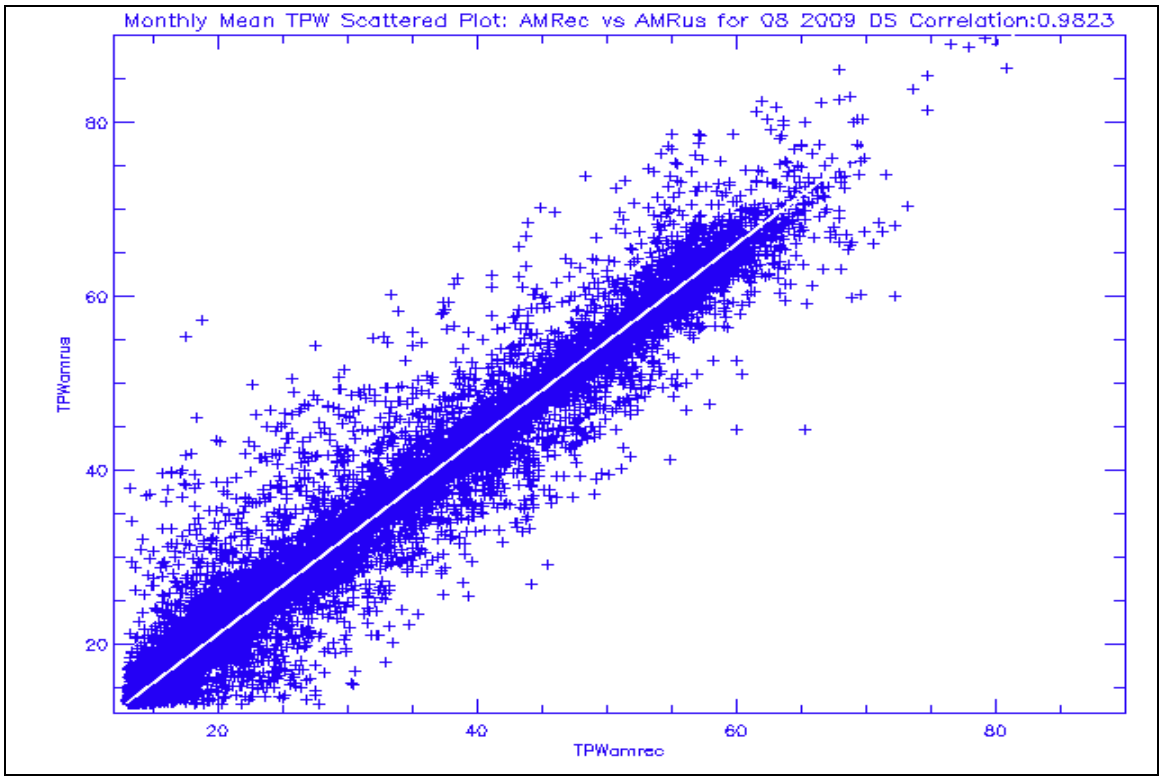


**Figure 27 Monthly TPW Correlation between AMRus and AMRec Dec August 2009**

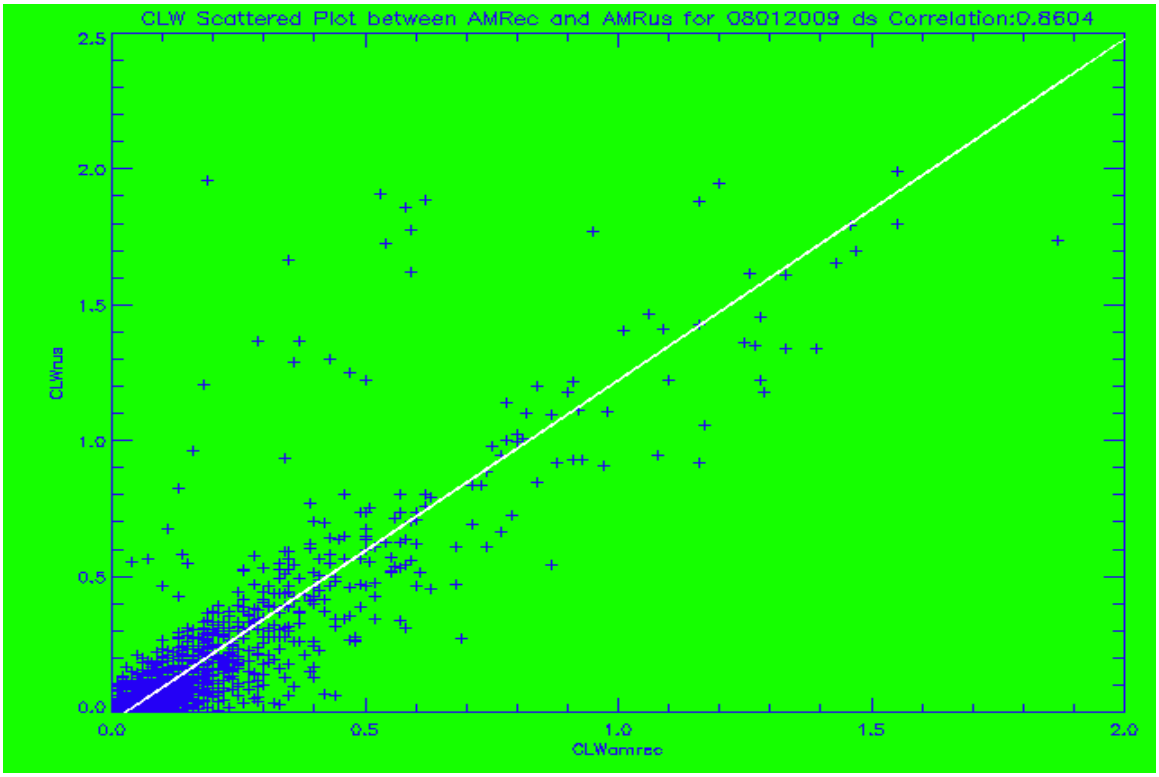


**Figure 28a Daily CLW Correlation between AMRus and AMRec Dsc 08012009**

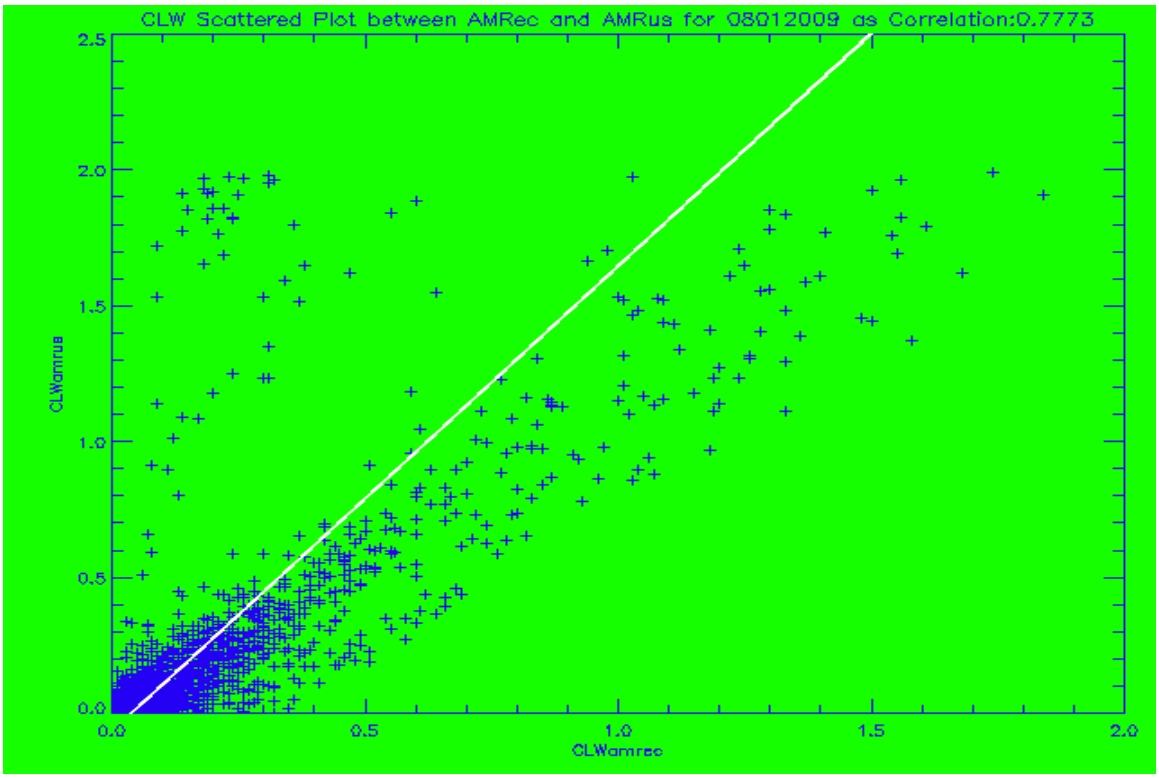


**Figure 28b Daily CLW Correlation between AMRus and AMRec Asc 08012009**

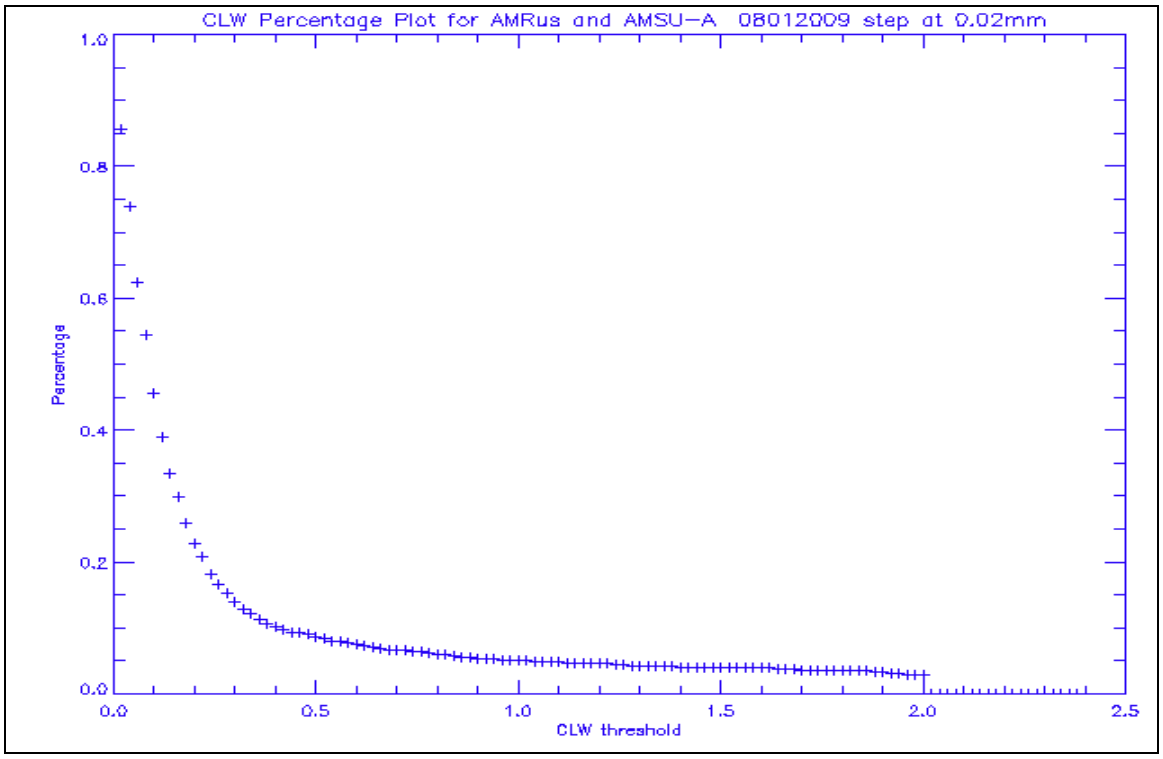


**Figure 29a CLW percentage between AMSU-A and AMRus: The X-axes is the cloud existence threshold from 0 to maximum CLW at 2.5 mm. The Y-axes is the percentage of points where both retrievals are higher than the threshold with respect to all retrieved points. 08012009**

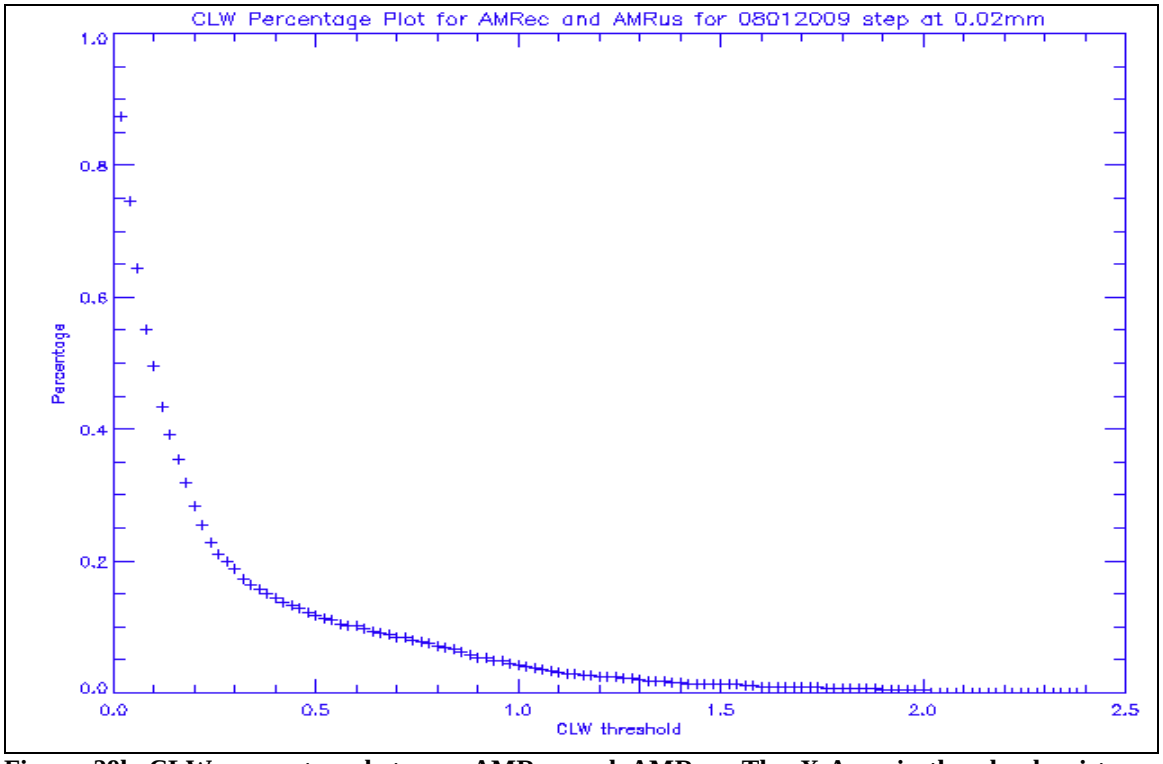


**Figure 29b CLW percentage between AMRec and AMRus: The X-Axes is the cloud existence threshold from 0 to maximum CLW at 2.5 mm. The Y-Axes is the percentage of points where both retrievals are higher than the threshold with respect to all retrieved points. 08012009**